Experimental techninque of Underground Physics

Main recipes for the Dark Matter particle direct detection

- Underground site
- Low bckg hard shields against γ's, neutrons
- Lowering bckg: selection of materials, purifications, growing techniques, ...
- Rn removal systems

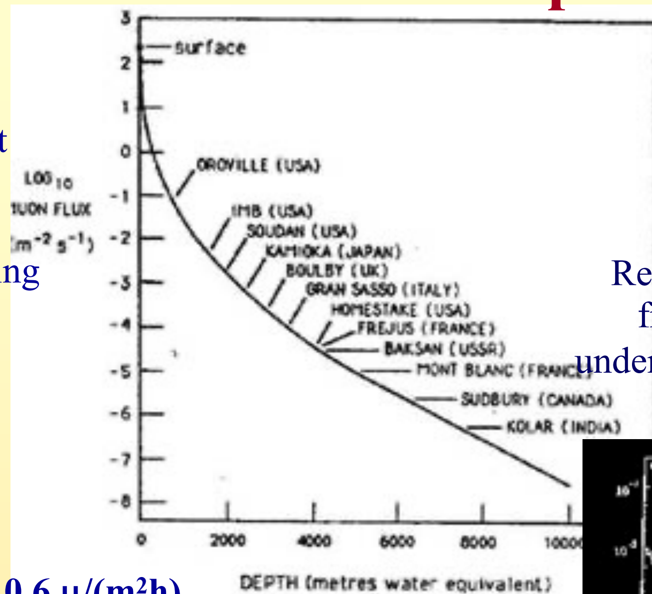

Reduction from the underground site

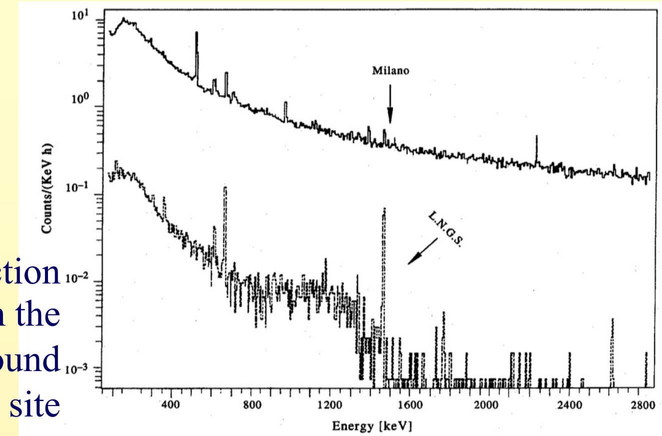

Background sources

- Background at LNGS:

muons	→	**0.6 μ/(m²h)**
neutrons	→	**1.08·10⁻⁶ n/(cm²s) thermal**
		1.98·10⁻⁶ n/(cm²s) epithermal
		0.09·10⁻⁶ n/(cm²s) fast (>2.5 MeV)
Radon in the hall	→	**≈30 Bq/m³**

- Internal Background:

selected materials (Ge, NaI, AAS, MS, ...)

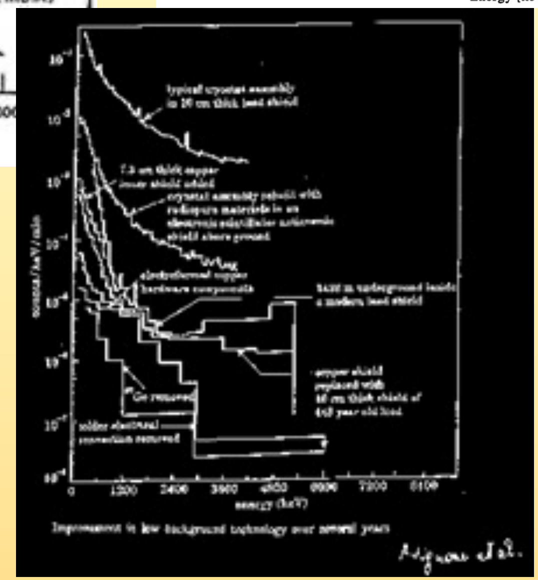

Example of background reduction during many years of work

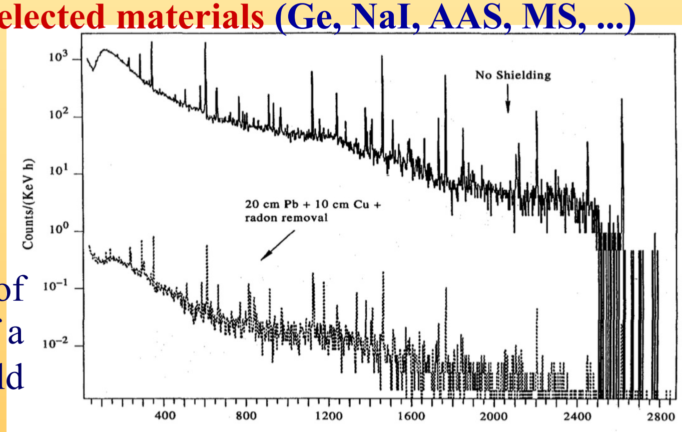

Example of the effect of a passive shield

Shielding

Passive shield: Lead (Boliden [< 30 Bq/kg from ^{210}Pb], LC2 [<0.3 Bq/kg from ^{210}Pb], lead from old roman galena), OFHC Copper, Neutron shield (low A materials, n-absorber foils)
Active shield: Low radio-activity NaI(Tl) surrounding the detectors

Dark Matter direct detection activities in underground labs

- Various approaches and techniques
- Various different target materials
- Various different experimental site depths
- Different radiopurity levels, etc.

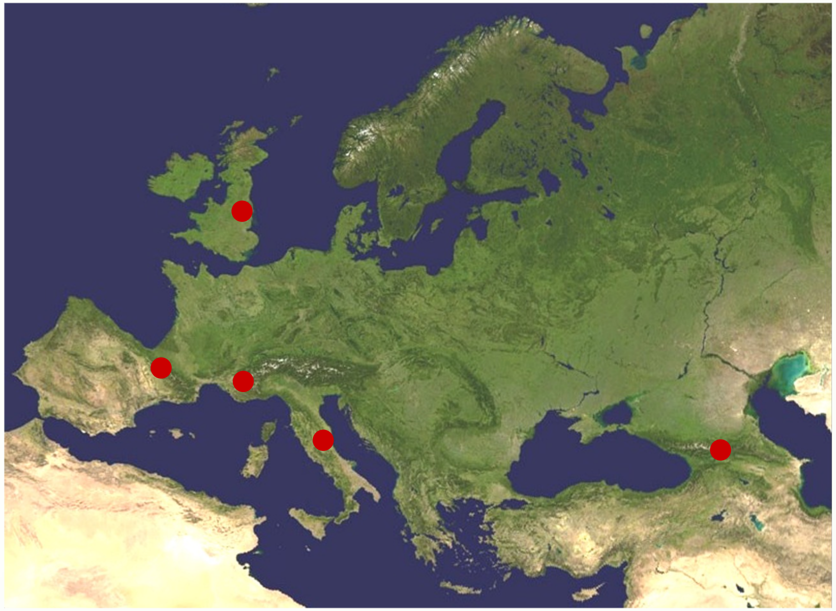

- Gran Sasso (depth ~ 3600 m.w.e.): DAMA/NaI, DAMA/LIBRA, DAMA/LXe, HDMS, WARP, CRESST, CUORE, XENON, DarkSide, SABRE, Cosinus, NEWSdm, CYGNO
- Boulby (depth ~ 3000 m.w.e.): DRIFT, Zeplin, NAIAD
- Modane (depth ~ 4800 m.w.e.): Edelweiss, DAMIC-M
- Canfranc (depth ~ 2500 m.w.e.): ANAIS, Rosebud, ArDM

- SNOlab (~ 6000 m.w.e.): Picasso, Coupp, PICO, DEAP, CLEAN, SuperCDMS, DAMIC, NEWS-G
- Stanford (~10 m): CDMS I
- Soudan (~ 2000 m.w.e.): CDMS II, SuperCDMS, CoGeNT
- SURF (~4400 m.w.e.): LUX-Zeplin, MALBEK
- WIPP (~1600 m.w.e.): DMTPC
- South Pole: DM-ICE

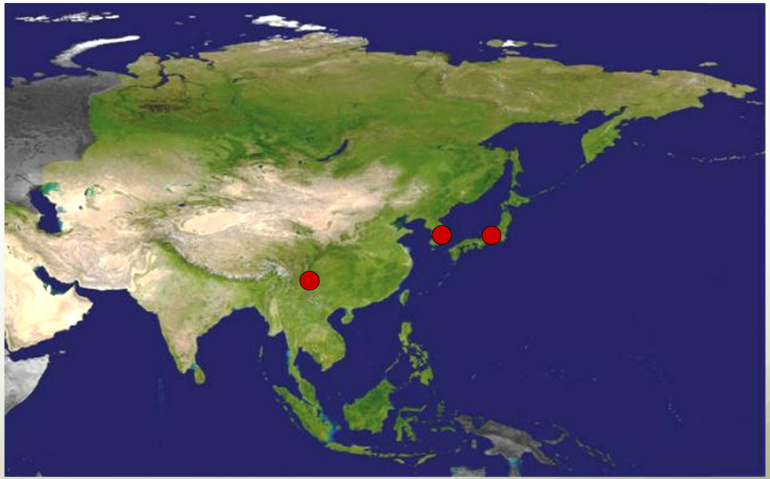

- Y2L (depth ~ 700 m): COSINE-100/KIMS
- KAMIOKA: PICO-LON, NEWAGE, XMASS
- CJPL (depth ~6700 m.w.e.): Texono, CDEX, PANDAX

I raggi cosmici in superficie

- A livello del mare siamo continuamente investiti da circa 200 particelle per m^2 e per s, i cosiddetti **"raggi cosmici"**
  - Sono il prodotto dell'interazione di protoni di alta energia provenienti dallo spazio
  - Sono stati il primo acceleratore naturale per lo studio delle particelle elementari

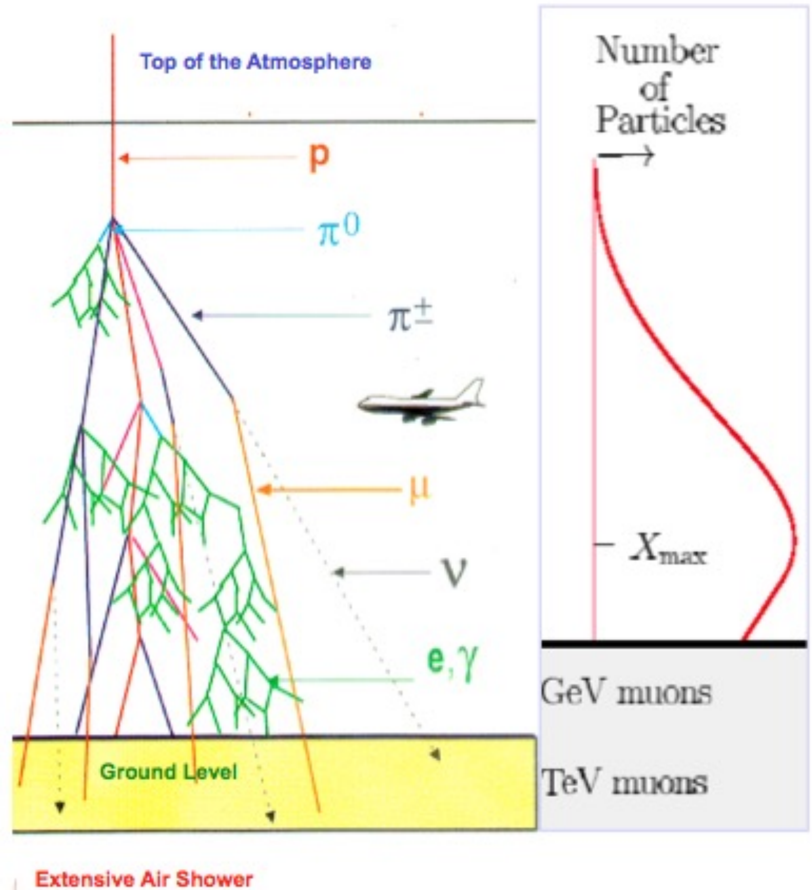

I raggi cosmici in superficie

- A livello del mare siamo continuamente investiti da circa 200 particelle per m^2 e per s, i cosiddetti **"raggi cosmici"**
  - Sono il prodotto dell'interazione di protoni di alta energia provenienti dallo spazio
  - Sono stati il primo acceleratore naturale per lo studio delle particelle elementari

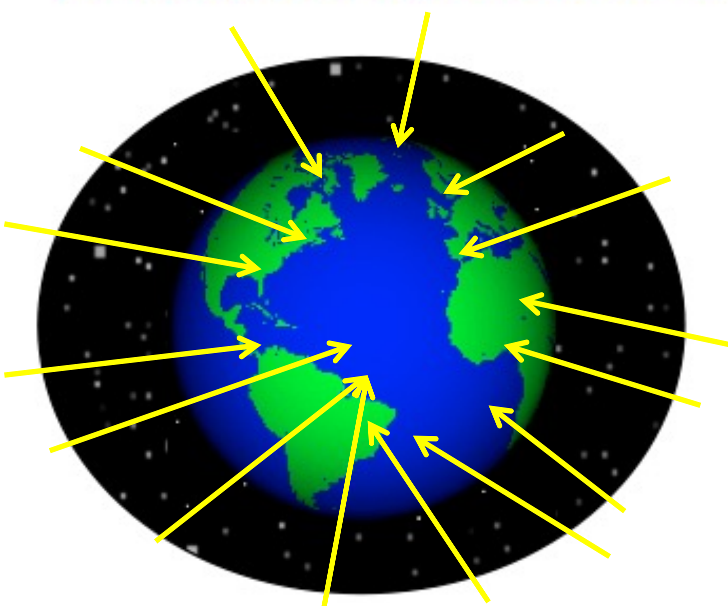

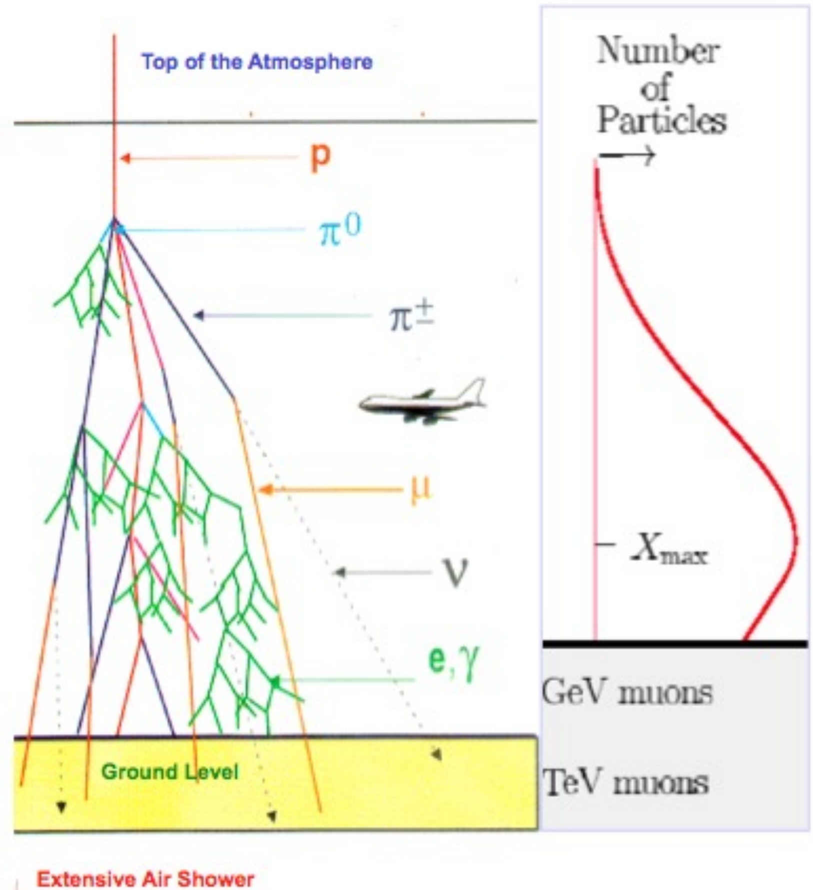

Muon flux underground

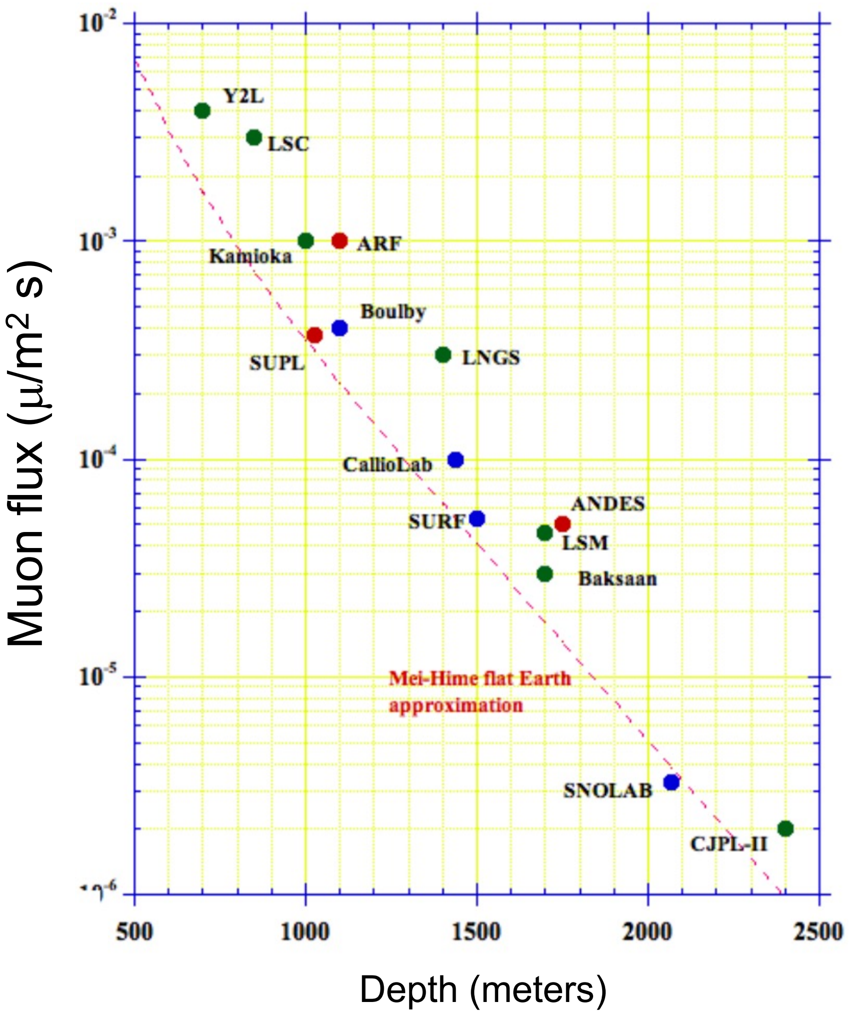

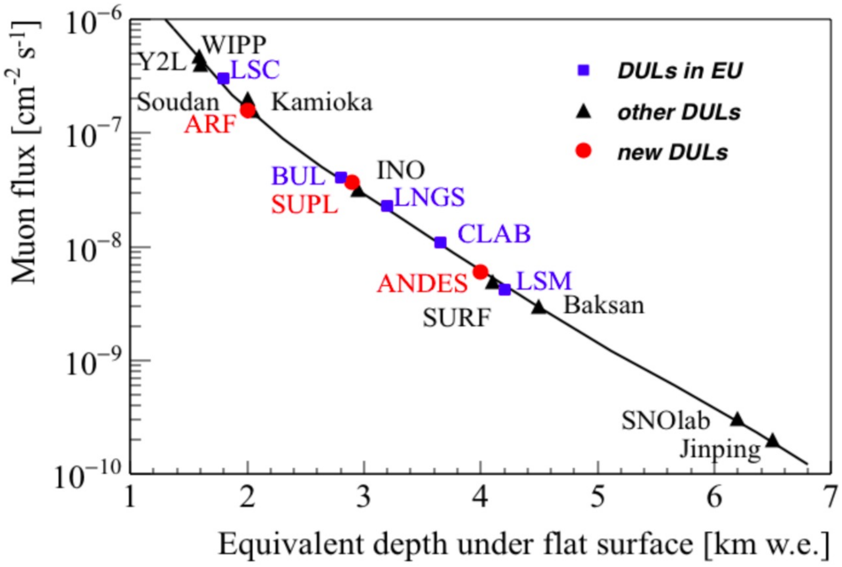

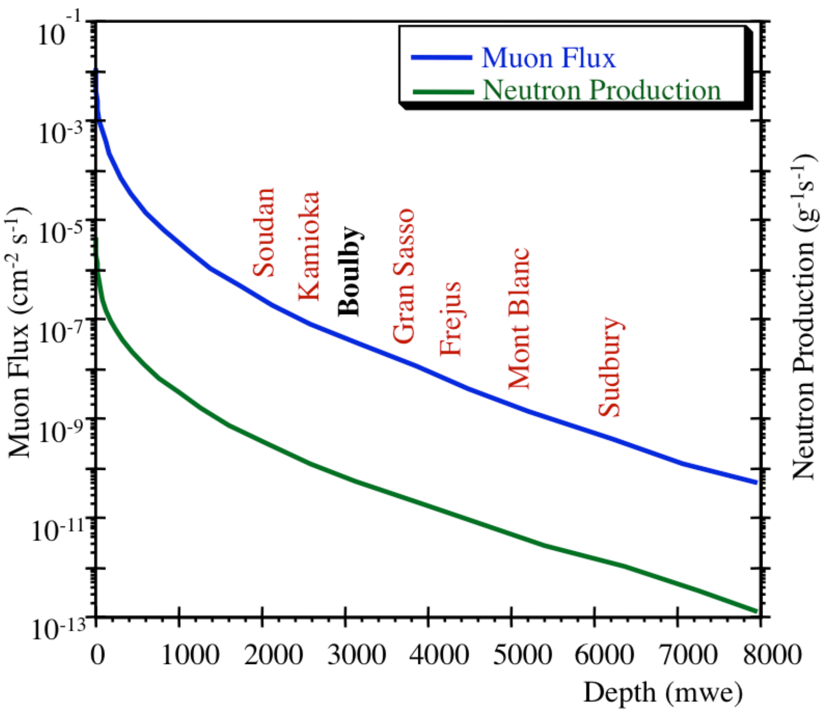

Muon flux underground

- Under a flat surface (SNOLab, CallioLab,SURF)
- Under a mountain (Baksan, LNGS, LSC, LSM, CJPL)
- Underground cosmic-ray muons angular dependence can be important

Muon data for LNGS: MACRO and Borexino

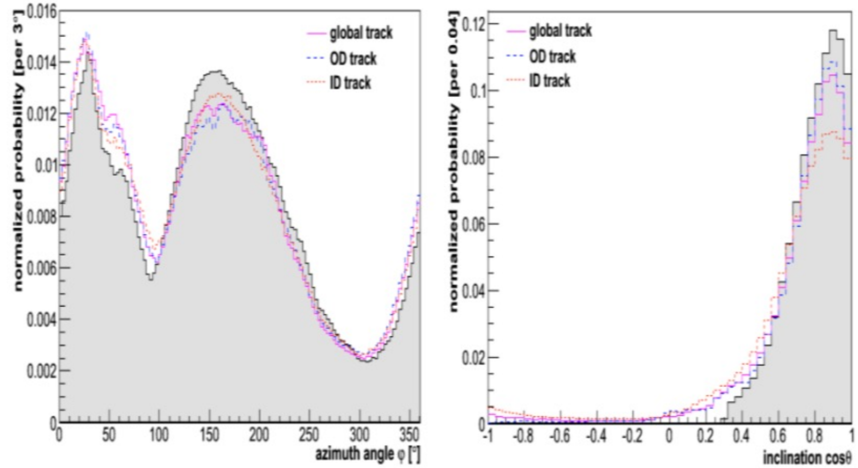

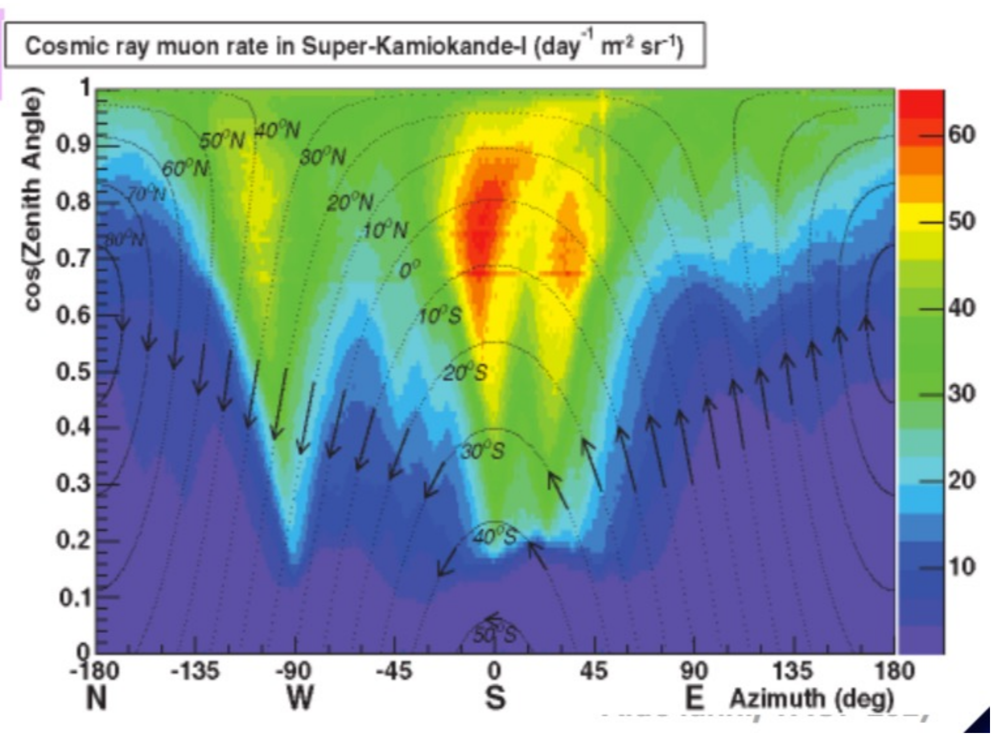

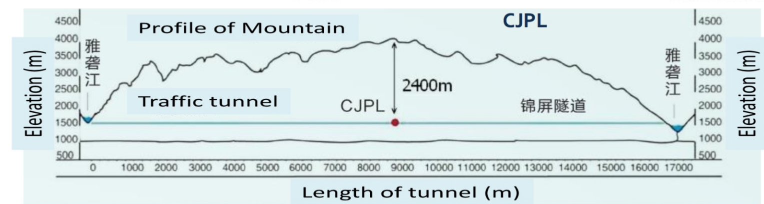

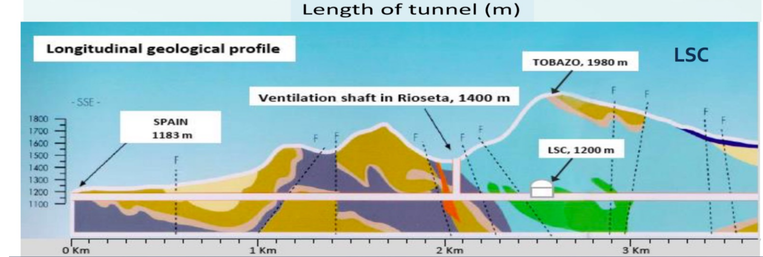

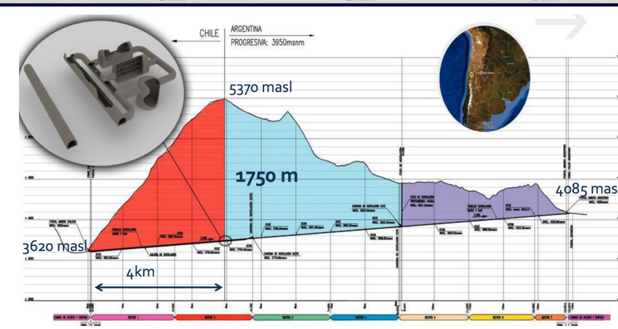

Cleanliness

- **Mine environment or small volume underground area**
  - Specific protocol to enter lab area (SNOLab, Boulby, SURF,SUPL)
  - With some basic protocol it is possible to achieve good conditions
    - SNOLab class 2000 or better throughout the whole volume with a more demanding protocol
    - SURF class ~3000
    - BOULBY main area ISO7
    - All: dedicated personnel for regularly cleaning activity
- **Large volume, not mine environment** (LNGS, CJPG)
  - Specific protocol in sectors (clean rooms)
- **Medium size volume, not mine environment** (LSC,LSM)
  - Specific protocol (cleaning shoes, regular floor cleaning …)
  - Example: at the LSC particulate counting in different areas ~ ISO7

Main supporting facilities

- **HPGe screening facilities** (in all labs) + alpha counting + ICP-MS
- **Cu electro-forming production** (SURF, LSC, CJPL,SNOLab,ARF)
- **Clean rooms** (ISO5, ISO6)
- **Radon abatement systems** (1000x Rn reduction)
  - In operation at LNGS, LSC, Y2L, LSM (100 – 300 m^3/h)
  - To be installed at SURF, SNOLab,CJPL, SUPL, ARF
- **Radon-free clean rooms**
  - Present at LNGS
  - To be installed at SURF, SNOLab …
- Sensitive **radon detectors** (<mBq/m^3) for emanation and monitoring
  - Monitoring blanket N2 gas in the Borexino-CTF, Xenon1t water tanks …
- Crystal growing facility (ARF,CJPL)

Main supporting facilities: HPGe screening facilities

	SNOLab	LNGS	LSC	SURF	LSM	Boulby	Baksan	Kamioka	CJPL
Number of HPGe detectors	5	12(+1)	7	4+1	18+6	4+3	2+2	6	10

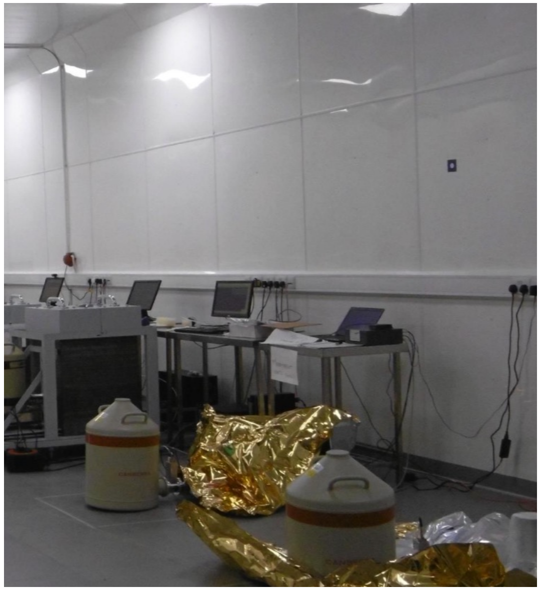

- ✓ Sensitivities
  - Commercial detectors 0.5 – 1 mBq/kg in U, Th
  - Custom 10-50 μBq/kg
- ✓ Overall DULs have collected some 81 HPGe which corresponds to about 8 M€
- ✓ These detectors used to support screening for experiments and environmental research and other requests from Research Institutions not directly related to DULs

HPGe detectors at LNGS

HPGe detectors at SURF, ISO6

DULs as multidisciplinary Research Infrastructures

+ Geophysics

- Underground environment enhance the sensitivity to local and global phenomena using data from strain meters and seismometers
  - ✓ Local: slow earthquakes, hydrogeologically-induced deformations, sesonal charge and discharge of aquifiers, ocean loading tides
  - ✓ Global: free oscillations of the Earth induced by large quakes, background free oscillations due to atmospheric environment, free core nutation …
- Ring laser in underground for Lense-Thirring effect measurement

- DULs could provide data from different locations worldwide
- Muon tomography for deep geological mapping applications

GINGERino: deep underground ring laser

GINGER-ino (INFN-LNGS)+ Seismometers (INGV)

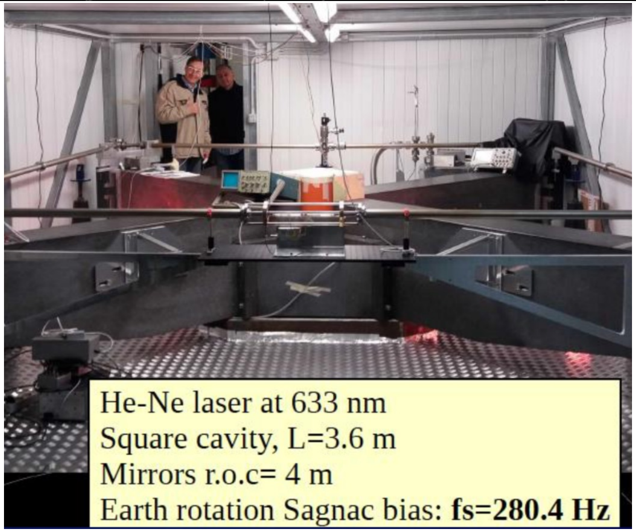

+ Biology

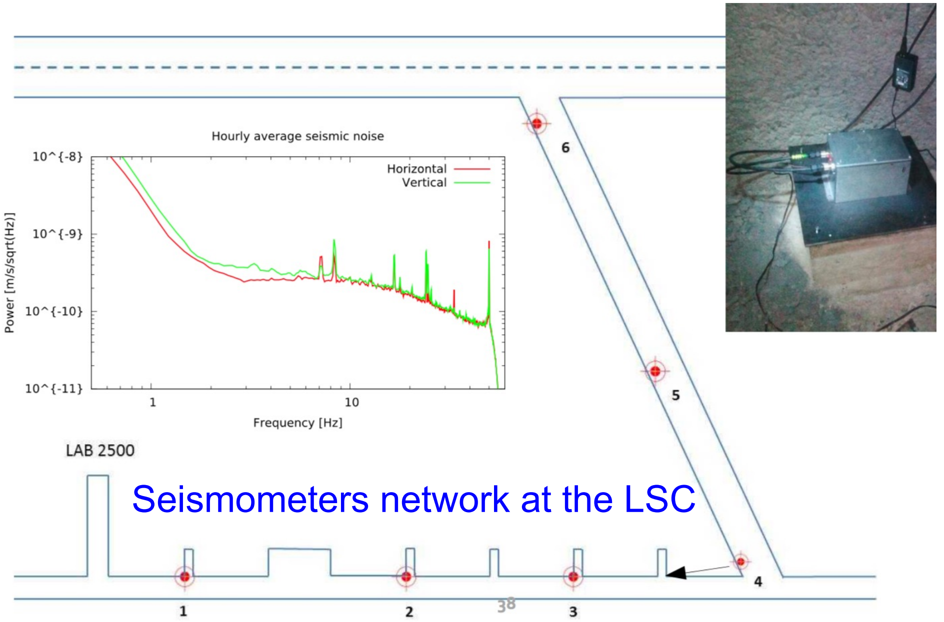

The European underground facilities

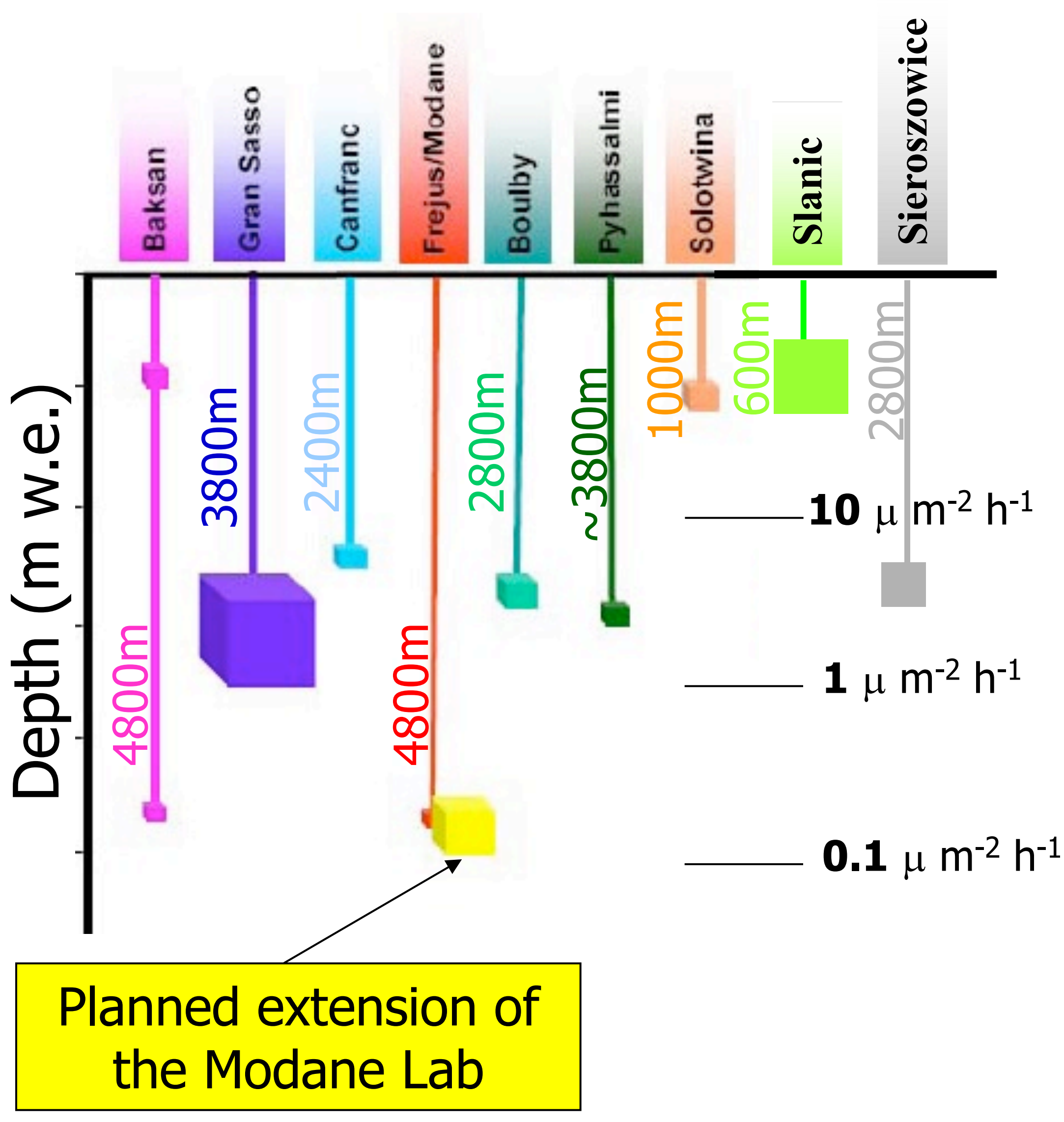

Baksan, RU
Gran Sasso, IT
Modane, FR
Canfranc, ES
Boulby, UK
Pyhäsalmi, FIN
Sieroszowice, PL
Slanic, RO
Solotvina, UKR

The origin of radiation

- Our galaxy's stock of heavy elements was mostly produced in supernovae explosions that eject stable and unstable nuclei into the interstellar medium.
- The interstellar clouds containing these elements may later condense to form stellar systems. By the time this happens, most of the short-lived nuclei would have decayed, so planets contain, at their birth, only nuclei with life-times greater than, say, 10^6 yr.
- On Earth, $\sim 4.5 \times 10^9$ yr after its formation, most of the original unstable nuclei have decayed leaving only those with $T_{1/2} > 10^8$ yr.
- There is also continuous production of unstable nuclei by cosmic-rays entering the Earth's atmosphere.
- The α and β decays of these nuclei constitute the **natural radioactivity** that was discovered by Becquerel at the end of the nineteenth century.
- All living species have evolved in this bath of radiation.
- What is new on Earth is the existence of an artificial radioactivity due to the development of nuclear technologies, most importantly energy production by nuclear reactors.
- There are now also numerous uses of radioactive nuclei, most notably in medical treatment and dating.

Fossil radioactivity (2)

- Most radioactive nuclei were produced in supernovae that generate a mix of neutron-rich nuclei in a period of time of order a few seconds. When, some millions of years later, the cloud condensed to form the solar system, a few radioactive nuclear species were still present.
- At the present epoch, only nuclei with **mean lives greater than**, say, 10^8 yr, are still present in significant numbers.
- These long-lived nuclei involve either highly forbidden β decays (large spin changes) or are α-decays that happen to have Q-values that place the half-lives in this range.

Nuclei with 10^8 yr < $T_{1/2}$ < 10^{12} yr.

The "isotopic abundance" is for the terrestrial mix and the activity for the purified element corresponds to the terrestrial isotopic mix. For the activity in the Earth's crust, the uranium and thorium activities include the activities of the daughters. Note that three nuclides, ^{40}K, ^{146}Sm and ^{235}U have lifetimes much less than the age of the Earth (~4.5 × 10^9 yr) and therefore have very small isotopic abundances.

decay	half-life (years)	isotopic abundance (percent)	activity ($Bq\,kg^{-1}$) (element)	activity ($Bq\,kg^{-1}$) (crust)
$^{40}K \to {}^{40}Ca\, e^- \bar{\nu}_e$ 89% $\to {}^{40}Ar\, \nu_e$ 11%	1.28×10^9	0.0117	3.0×10^4	6.3×10^2
$^{87}Rb \to {}^{87}Sr\, e^- \bar{\nu}_e$	4.75×10^{10}	27.83	8.8×10^5	8.0×10^1
$^{146}Sm \to {}^{142}Nd\, \alpha$	1.03×10^8	$< 10^{-7}$	< 1	$< 10^{-4}$
$^{147}Sm \to {}^{143}Nd\, \alpha$	1.06×10^{11}	15.1	1.3×10^5	9×10^{-1}
$^{176}Lu \to {}^{176}Hf\, e^-$	3.78×10^{10}	2.61	5.5×10^4	4×10^{-2}
$^{187}Re \to {}^{187}Os\, e^- \bar{\nu}_e$	4.15×10^{10}	62.6	1.1×10^6	8×10^{-4}
$^{232}Th \to {}^{228}Ra\, \alpha$	1.405×10^{10}	100	4.05×10^6	3.5×10^2
$^{235}U \to {}^{231}Th\, \alpha$	7.038×10^8	0.72	5.7×10^5	1.7×10^1
$^{238}U \to {}^{234}Th\, \alpha$	4.468×10^9	99.275	1.2×10^7	4.7×10^2

L’origine della radiazione

Radiazione cosmica:

Raggi cosmici primari

Raggi cosmici secondari

Radioattività naturale:

Radionuclidi isolati

Famiglie radioattive naturali

Radioattività artificiale.

La radioattività naturale può essere divisa in:

- radioattività “***fossile***” dovuta ad elementi presenti alla formazione della Terra
- radioattività “***cosmogenica***” dovuta ad elementi continuamente prodotti nell’atmosfera dai raggi cosmici.

Le tecniche per produrre radioattività artificiale possono essere divise in quelle che usano neutroni (attivazione da neutroni) e quelle che usano fasci di particelle cariche.

Sources of background

a) environmental radioactivity
b) radioactive impurities in detector and shield material
c) Rn and its progenies
d) cosmic rays
e) neutrons from natural fission and (α, n) reactions

Examples:

Background components in Ge spectrometry

- external gamma radiation (2.6 MeV ^{208}Tl, {up to 3.2 MeV ^{214}Bi})
- radio-impurities close to crystal (primordial, anthropogenic)
- Rn and its progenies
- cosmic rays (neutrons, muon and activation)
- neutrons from fission and (α,n) reactions

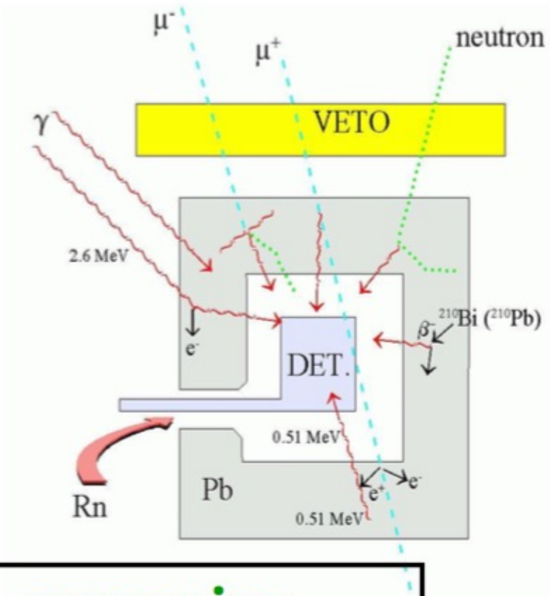

most important: material screening
U/Th chains and K dominant from Bq/kg down to μBq/kg only reliably radiopure material - Cu - but mBq/kg cosmogenics besides Si, Ge, Au, Ag, Hg, (Pb – except Pb-210)

G. Heusser

The neutrons induced by muons

induce depth dependence of background inducing muons and neutrons

- the integral **neutron yield** critically depends on the chemical composition and on the density of the medium through which the muons interact
- the dependence on atomic weight is well described by a power law: $Y = 4.54 \times 10^{-5} A^{0.81}$ neutrons per muon per g/cm^2
- alternatively, it can also be expressed as:

$Y = 1.27 \times 10^{-4} (Z^2/A)^{0.92}$ neutrons per muon per g/cm^2

- thus, the integral yield of neutrons produced by muons deep underground at LNGS is:
    - $Y \simeq (1–7) \times 10^{-4}$ neutrons per muon per g/cm^2 for relatively light nuclei
    - and $Y \simeq 4.5 \times 10^{-3}$ neutrons per muon per g/cm^2 for lead

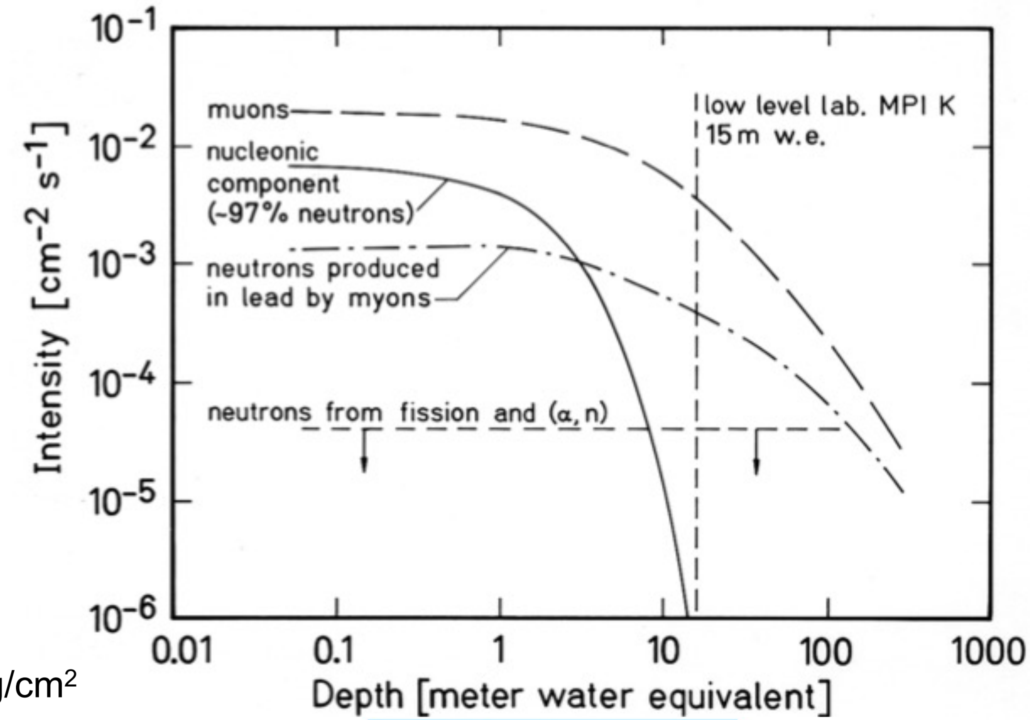

muon induced neutron flux

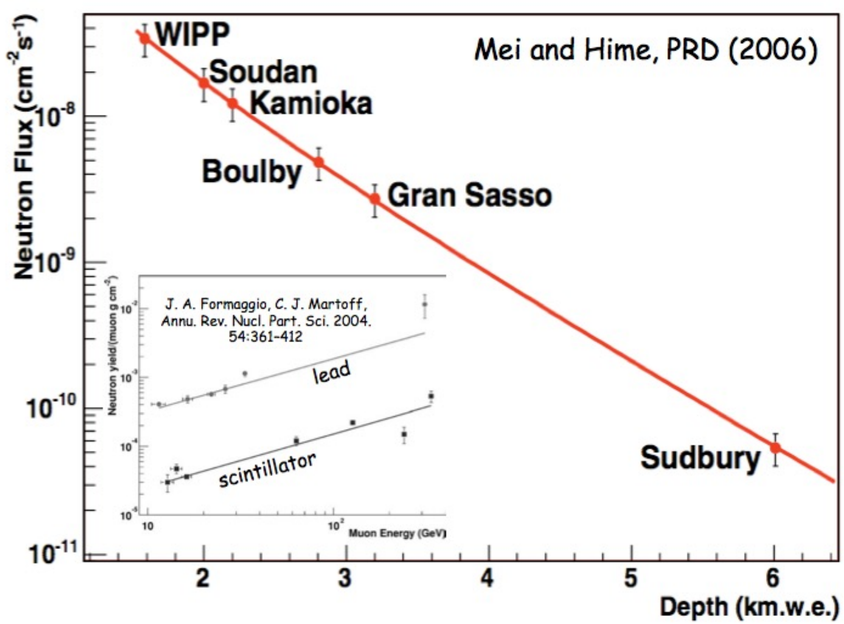

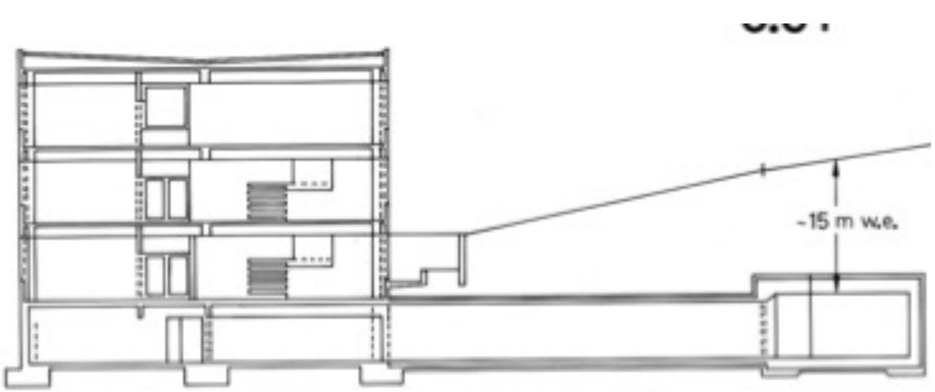

neutron attenuation

moderate !!!
plus capture ??

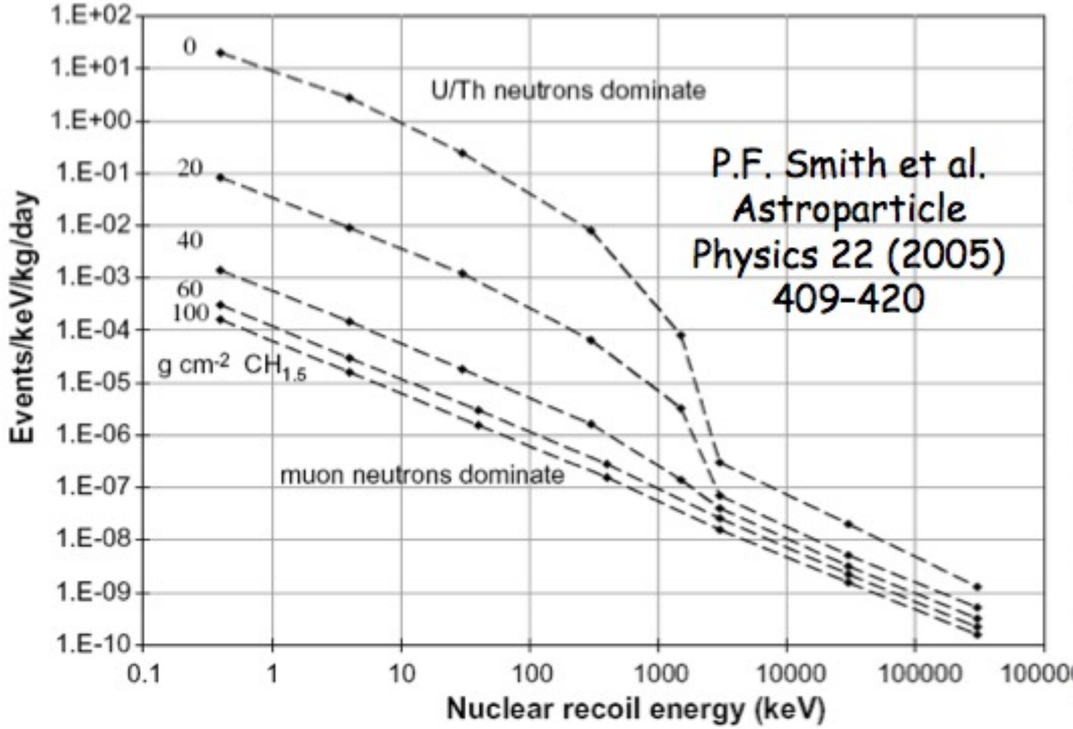

neutron background rate from U/Th and muons in NaCl rock
at depth 3000 m.w.e. versus hydrocarbon shielding thickness

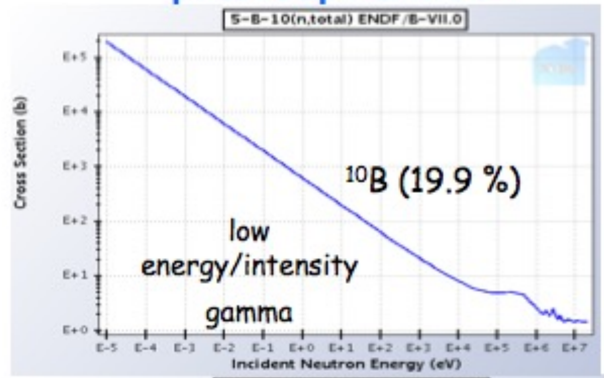

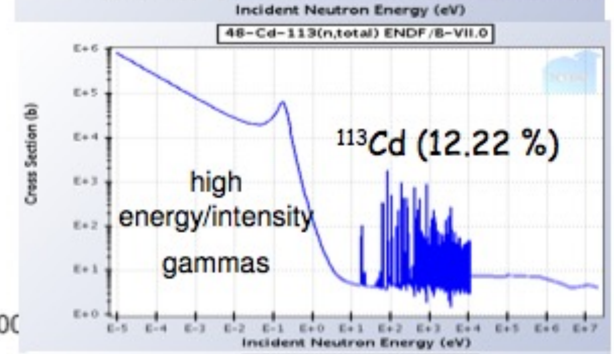

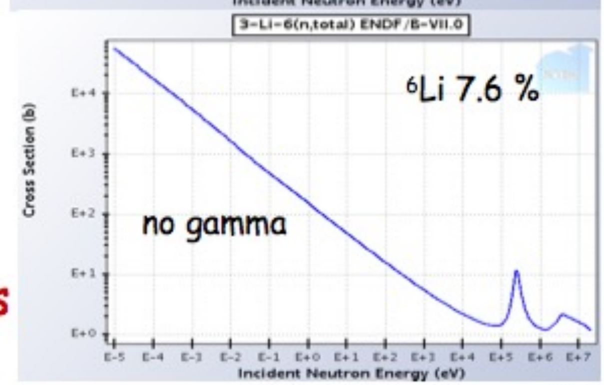

difficult to find radiopure n-capture compounds
with little mass substitution of the moderator

Neutron shields: low-A materials (paraffin, polyethylene, plastic, ...) for moderation + foils/materials (B, Cd, Li, ...) for n-capture

Cosmogenic radioactivity

- When cosmic-rays enter the Earth's atmosphere, they lose energy through ionization and nuclear reactions.
- The Earth's atmosphere is sufficiently thick that most of the primary cosmic-radiation stops in the atmosphere.
- Most cosmic radiation that reaches the Earth's surface consists of muons and neutrinos from the decays of pions produced in these collisions.
- A small nuclear component consisting mostly of neutrons reaches the surface but is quickly absorbed in the first few meters of the Earth's crust.
- Cosmic-rays produce radioactive nuclei via their interactions with nuclei in the atmosphere and in the Earth's crust.

- In **atmosphere**, the most common radioactivity produced is that of ^{14}C (and tritium).
- This nucleus is a secondary product of neutrons who are themselves produced by high-energy cosmic-ray protons that breakup nuclei in the atmosphere.
- The neutrons then either decay or are absorbed. The most common absorption process is the exothermic (n,p) reaction on abundant atmospheric nitrogen:

$$n + {}^{14}N \rightarrow p + {}^{14}C \quad T_{1/2}({}^{14}C) = 5730yr$$

- The produced ^{14}C is mixed throughout the atmosphere and enters the food chain through CO_2 ingesting plants. This results in a ^{14}C abundance in live organic material of about 10^{-12} relative to non-radioactive carbon. The resulting activity is about 250 Bq/kg.
- This allows the estimation of ages of dead organic material.

- High energy cosmic rays also produce radioactive nuclei through "**spallation**" reactions where one or more nucleons are removed from a nucleus.
- For example a neutron with kinetic energy greater than ~ 20 MeV can remove two nucleons from a germanium nucleus, e.g.

$$n + {}^{70}Ge \rightarrow 3n + {}^{68}Ge \quad T_{1/2}({}^{68}Ge) = 270.7day$$

- This reaction results in a radioactivity of 0.3 mBq/kg in germanium crystals produced at the Earth's surface.
- In high-purity germanium crystals used for detection of low-level radioactivity, it is the most important source of intrinsic radioactivity.
- If the crystals are placed underground, the production of ^{68}Ge ceases and the activity decays away.

Another example in Iodine:

$$n + {}^{127}I \rightarrow 3n + {}^{125}I \qquad T_{1/2}({}^{125}I) = 59.4\ d$$

(for NaI(Tl) it corresponds to 2.3 mBq/kg at surface)

- In rare circumstances, nucleons removed in spallation reactions can combine to form nuclei.
- For example the radioactive tritium isotope of hydrogen can be produced by cosmic rays by (for example) the reaction

$$n + {}^{16}O \rightarrow {}^{3}H + {}^{14}N \quad T_{1/2}({}^{3}H) = 12.35\text{yr}$$

- The atmospheric tritium combines with oxygen to form water that rains down on the Earth.
- Prior to the atmospheric testing of nuclear weapons and the Chernobyl reactor accident, this was the primary source of naturally occurring tritium.
- Because of its short half-life, tritium is absent in water from deep water reserves and also in crude oil.

^{129}I and ^{210}Pb

- ^{129}I ($T_{1/2}$ = 1.57×10^{7} yr) can be present in the natural Iodine with a percentage of the order of 1.5×10^{-12}
- ^{210}Pb long-lived isotope from ^{238}U chain

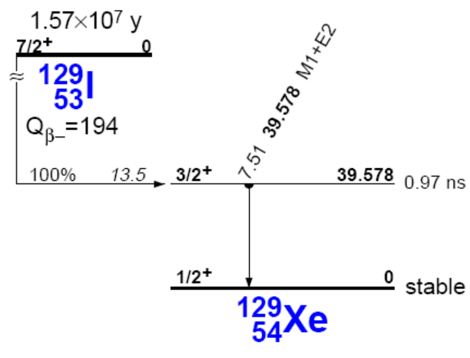

^{210}Pb: a= (7±4) μBq/kg $\quad$ ^{210}Pb: a= (29±3) μBq/kg

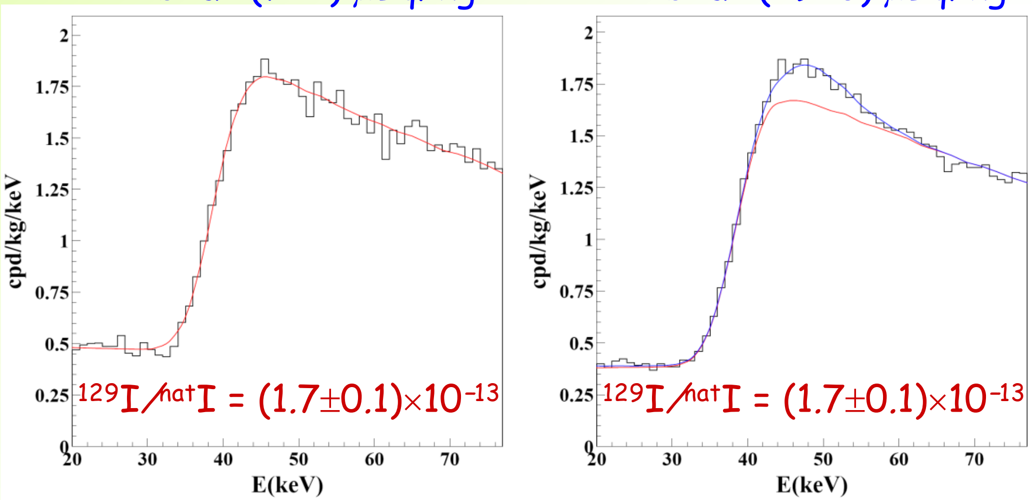

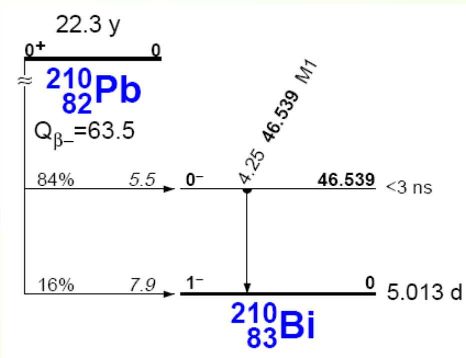

Energy distributions of two new DAMA/LIBRA detectors (histogram)
+ model of background for cosmogenic ^{129}I contribution (red lines)
+ contribution of internal ^{210}Pb (visible only in the second detector)

The amount of cosmogenic ^{129}I is at the same level ($\approx 1.7 \times 10^{-13}$) for all the new detectors
(if used for dating the NaI powders $\Rightarrow$ extracted from ore with an age of order of 50 Myr)

^{210}Pb in the new DAMA/LIBRA detectors typically ranges: (5 – 30) μBq/kg.

No sizeable surface pollution by Radon daugthers, thanks to the new handling protocols

... more on NIMA592(2008) 297

Example of cosmogenic activation in some detectors

For NaI(Tl) detectors the cosmogenic activation corresponds to 2.3 mBq/kg at the Earth's surface:

$n + {}^{127}I \rightarrow 3n + {}^{125}I$

${}^{125}I$ ($T_{1/2}$ = 59.4 d)

${}^{125}I \xrightarrow{EC} {}^{125}Te$

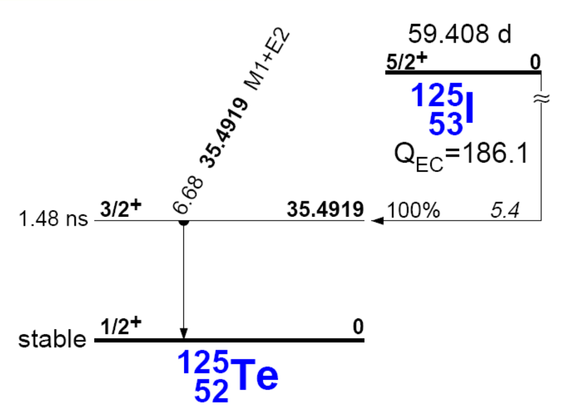

Detector just brought underground

April 03 *minus* July 04:

ΔT = 445 d vs $T_{1/2} \approx$ 60 days

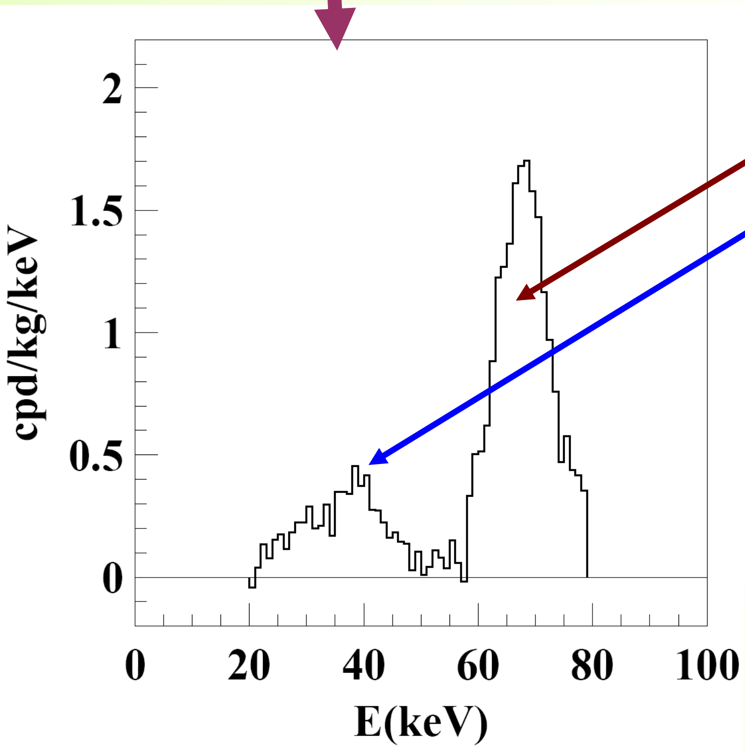

K shell (80.1%): E_{det} = 35.5 + 31.8 keV = 67.3 keV

L shell (15.6%): E_{det} = 35.5 + ≈ 4.6 keV ≈ 40 keV

M shell (≈4%): E_{det} = 35.5 + ≈ 0.8 keV ≈ 36 keV

Example of detector stored underground for longer time

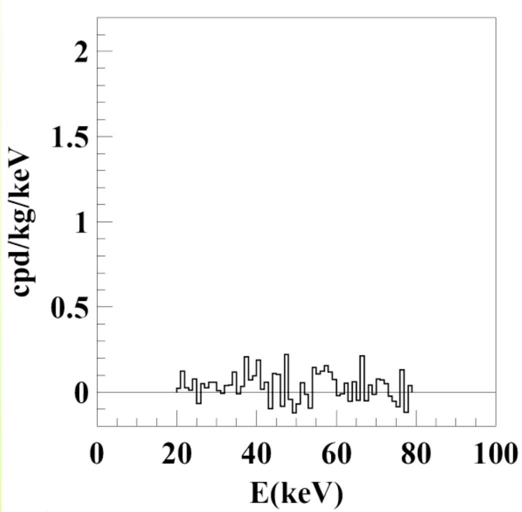

Cosmogenic radioactivity

$ZnWO_4$ and $CdWO_4$ crystal scintillators

^{65}Zn ($T_{1/2}$ = 245 d, Q_{EC} = 1352 keV) in $ZnWO_4$ crystal scintillator (0.5 mBq/kg)

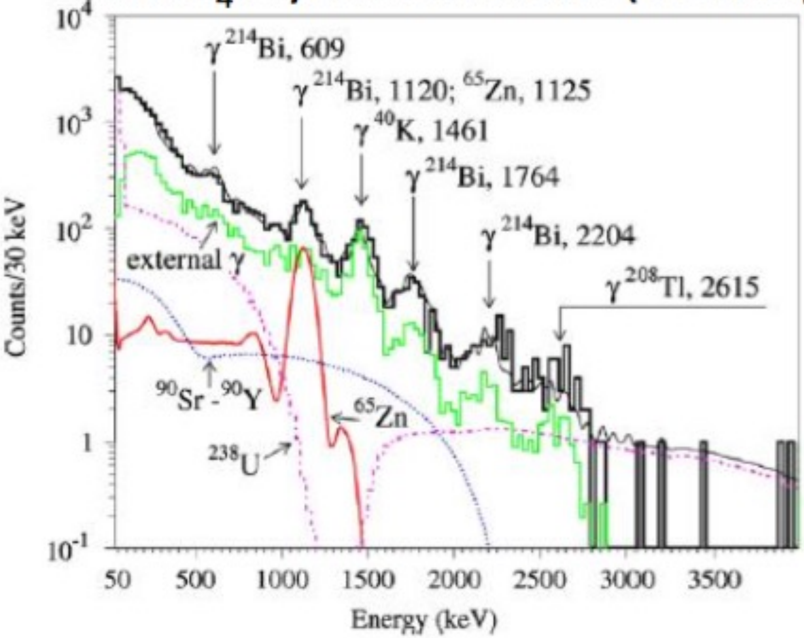

^{110m}Ag ($T_{1/2}$ = 250 d, Q_β=2893 keV) in $^{116}CdWO_4$ crystal scintillator

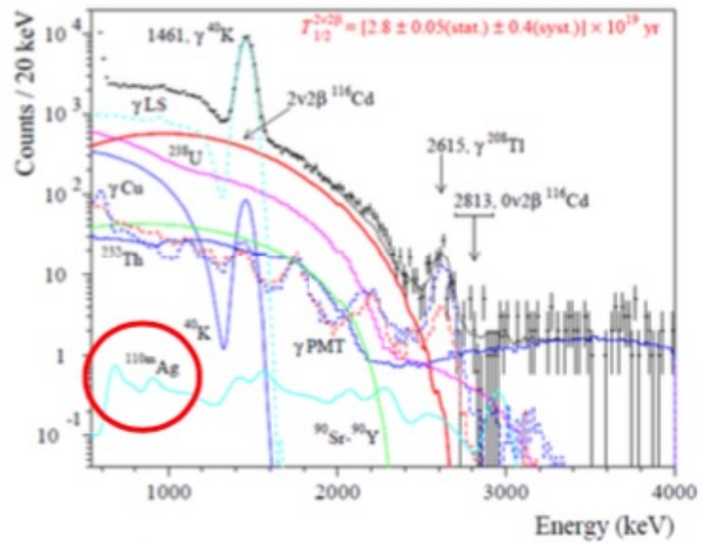

Monte Carlo simulation →

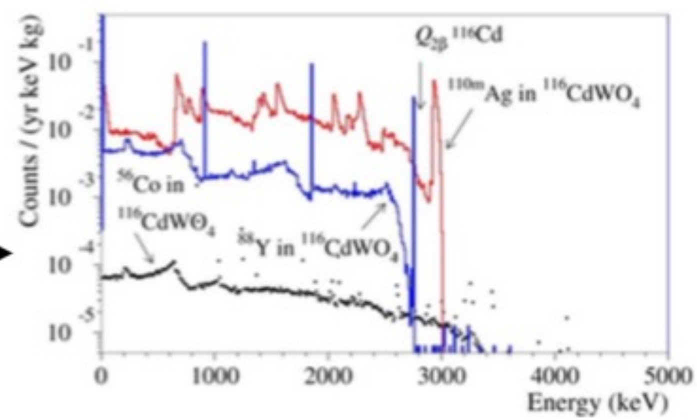

Cosmogenic activation in situ

Liquid scintillators (Borexino)

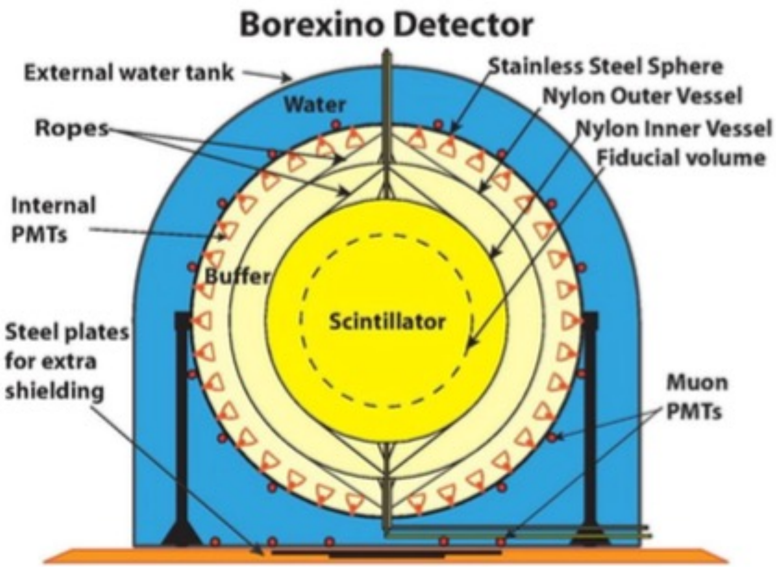

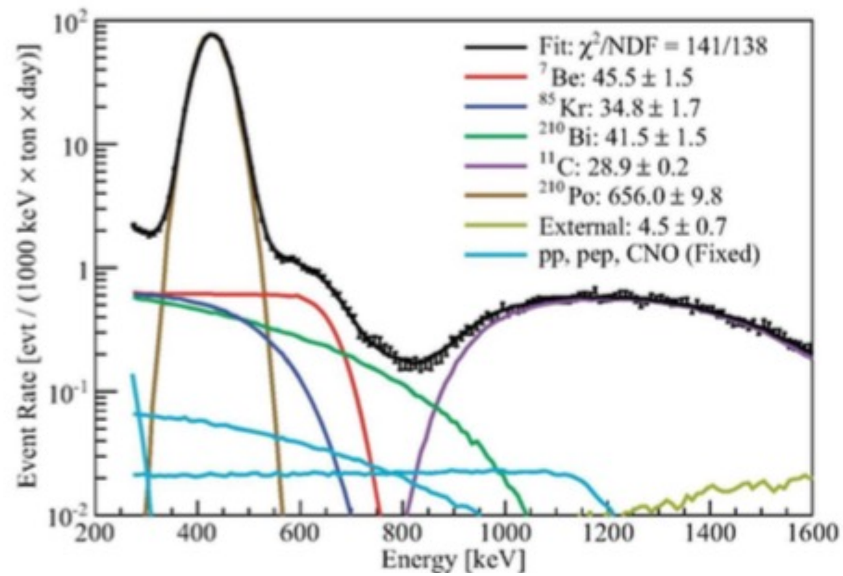

Cosmogenic Isotope	Lifetime	Q-Value [MeV]	Decay Type	Cosmogenic Isotope	Lifetime	Q-Value [MeV]	Decay Type
^{12}N	15.9 ms	17.3	β^-	^{6}He	1.16 s	3.51	β^-
^{12}B	29.1 ms	13.4	β^+	^{8}Li	1.21 s	16.0	β^-
^{8}He	171.7 ms	10.7	β^-	^{11}Be	19.9 s	11.5	β^-
^{9}C	182.5 ms	16.5	β^+	^{10}C	27.8 s	3.65	β^+
^{9}Li	257.2 ms	13.6	β^-	^{11}C	29.4 min	1.98	β^+
^{8}B	1.11 s	18.0	β^+				

La radioattività artificiale

Radionuclidi prodotti dall'attività umana, in seguito agli **<u>esperimenti nucleari</u>** negli anni cinquanta e sessanta, e per gli incidenti avvenuti alle centrali nucleari essenzialmente quelli di **<u>Three Mile Island</u>** <u>e di</u> **<u>Tchernobyl</u>**.

Principali radionuclidi di origine artificiale

Nucl	τ	Disintegrazione	γ (keV)		Nucl	τ	Disintegrazione	γ (keV)
^{90}Sr	28.6 a.	$<\beta^{+}>=196$ keV	202.5 479.5		^{137}Cs	30.1 a.	$<\beta^{+}>=188$ keV	661.6
^{131}I	8.02 j.	$<\beta^{+}>=182$ keV	284.3 364.5 637.1		^{134}Cs	2.06 a.	$<\beta>=157$ keV	563.2 569.3 604.7 795.8
^{95}Nb	34.9 j.	$<\beta^{+}>=43$ keV	765.8		^{106}Ru	372 j.	$<\beta^{+}>=10$ keV	511.9
^{140}Ba	12.7 j.	$<\beta^{+}>=251$ keV	29.9 162.7 537.3		^{133}Ba	10.5 a.	C.E.	276.4 302.9 359.1 383.9
^{125}Sb	2.73 a.		427.9 600.6		^{95}Zr	64 j.	$<\beta^{+}>=117$ keV	724.2 756.7
^{85}Kr	10.7 a.	$<\beta^{+}>=183$ keV	514.1		^{144}Ce	285 j.	$<\beta^{+}>=82$ keV	133.5
^{88}Kr	2.84 h.	$<\beta^{+}>=359$ keV	196.3 834.8 1529.8 2195.8 2392.1		^{136}Cs	13.2 j.	$<\beta^{+}>=100$ keV	176.6 273.6 340.6 818.5 1048.1 1235.3

Anthropogenic radioactivity

(appeared as result of human activity)

^{60}Co [1)]	γ	5.3 y
^{90}Sr - ^{90}Y [2)]	β	29 y
^{137}Cs, ^{134}Cs [2)]	γ	30 y, 2.1 y
$^{238,239,240,242}Pu$ [3)]	α	89 y, 24×10^3 y, 6.5×10^3 y, 3.7×10^3 y
$^{241,243}Am$ [3)]	α	432 y, 7370 y
^{244}Cm [3)]	α	18 y

1) production of steel

2) nuclear bomb tests; Chernobyl, Fukushima

3) Nuclear power stations; handling of nuclear materials; Chernobyl, Fukushima

Suppression of background

1) Underground laboratories
2) Shielding against Radon, its progenies and other airborne nuclides
3) External shielding
4) Material selection for detector construction
5) Limitation to the cosmic rays exposure
6) Active determination of background (PSD, other bckg identification techniques, id. of a Fiducial Volume …)
7) Coincidence techniques
8) Montecarlo simulations

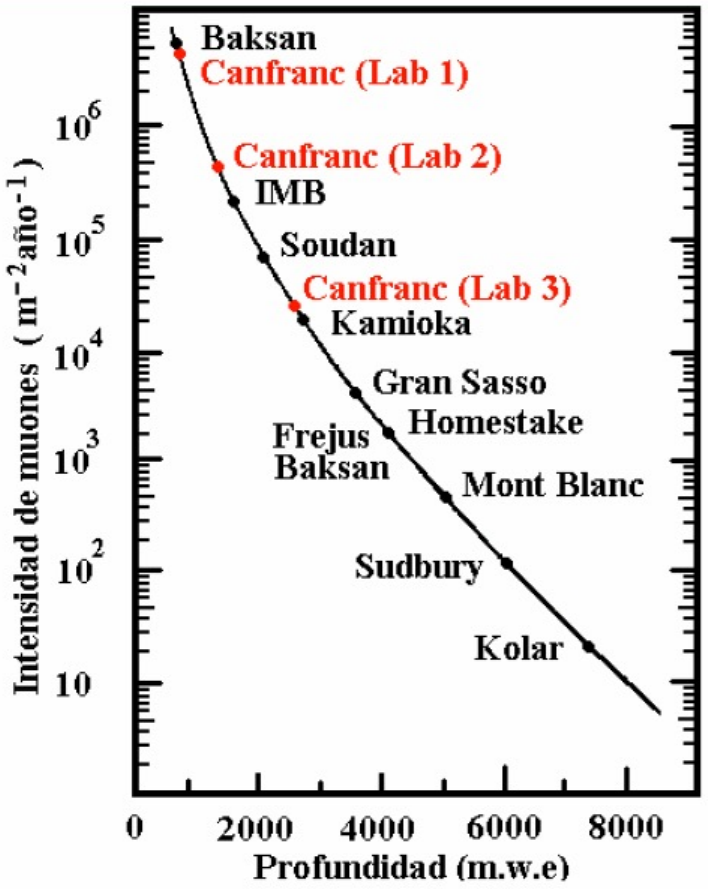

radioactive impurities in detector and shield material

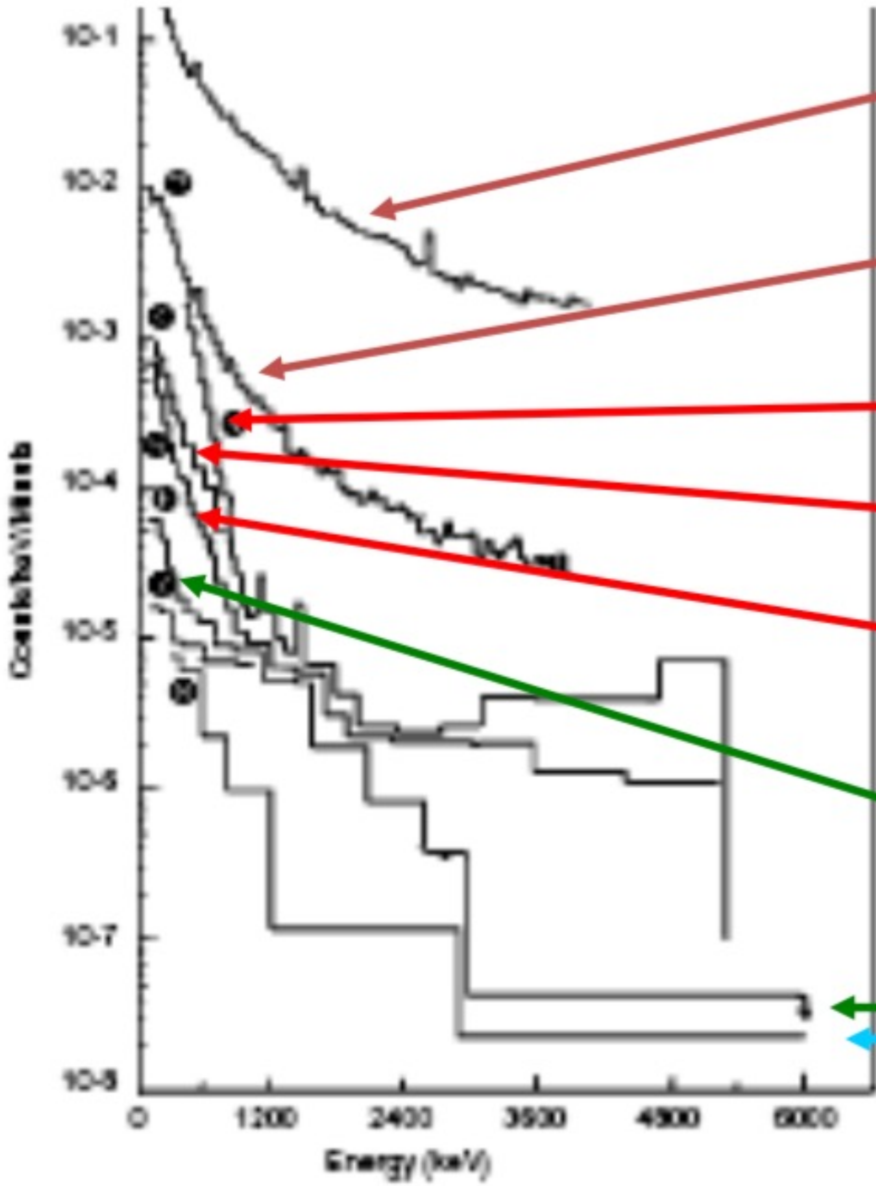

Ordinary cryostat + 10 cm of lead on surface

Low background cryostat + active scintillator (anti-coincidence)

1438 m underground

+ 7.3 cm of copper shield

The copper shield replaced by 10 cm of lead from Spanish galleon of 16 century

Indium contact is replaced

All the details replaced by OFHC copper

removed ^{68}Ge

background reduction by going underground

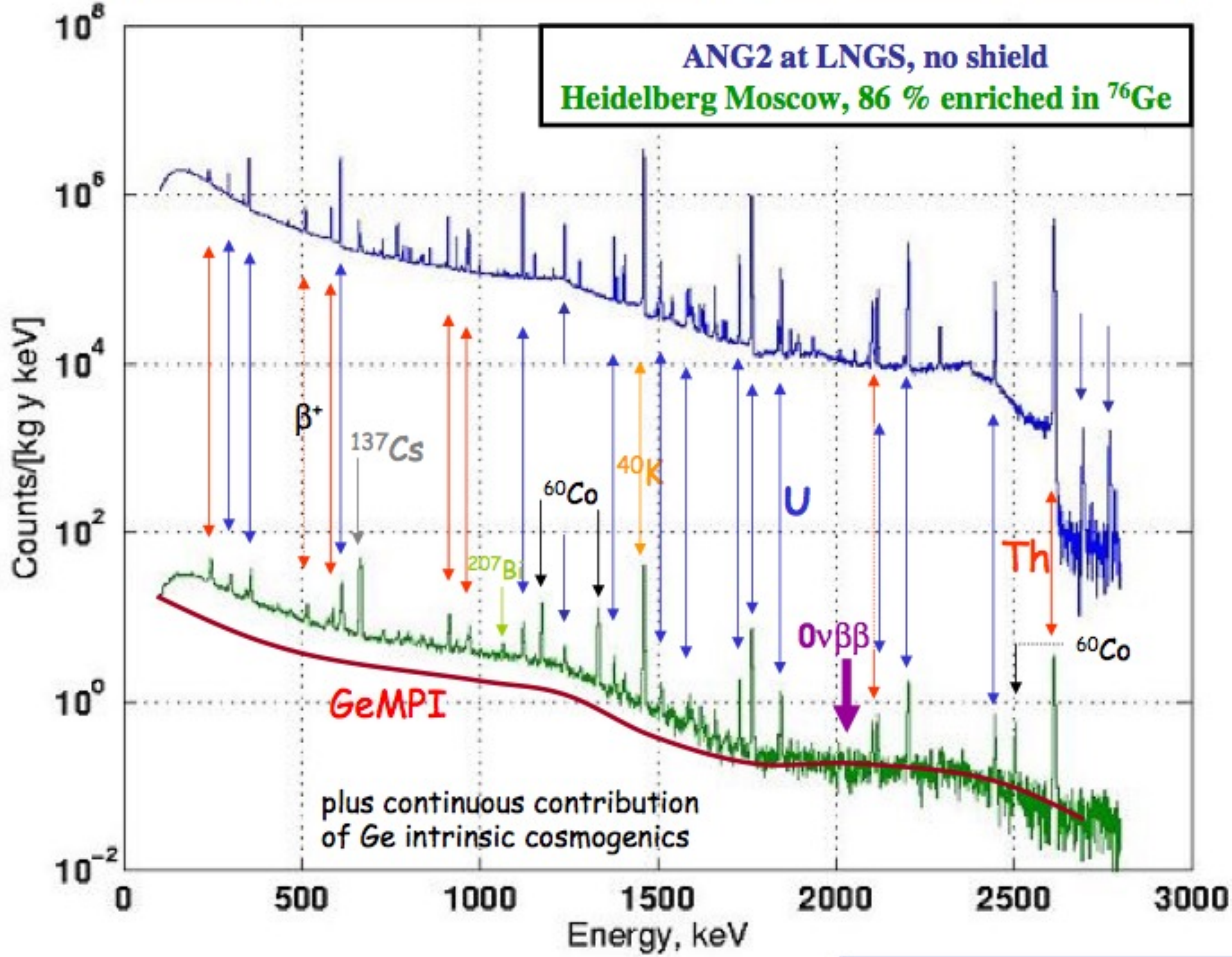

origin of background in Ge spectrometry

a) environmental gamma field

b) radio-impurities (primordial, anthropogenic, cosmogenic) in detector/shield material, and their surface

c) Rn and its progenies

d) interaction with cosmic rays

e) interaction with neutrons from fission and (α,n) reactions

choice and thickness of shielding material correlates with d) and e)

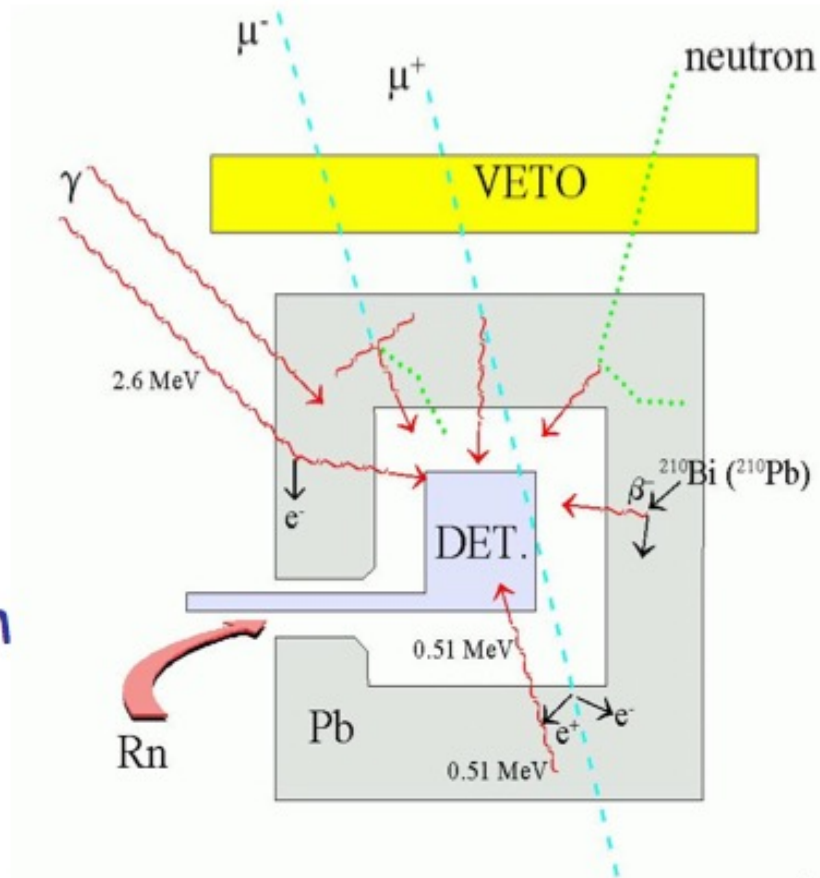

most important: material selection by screening

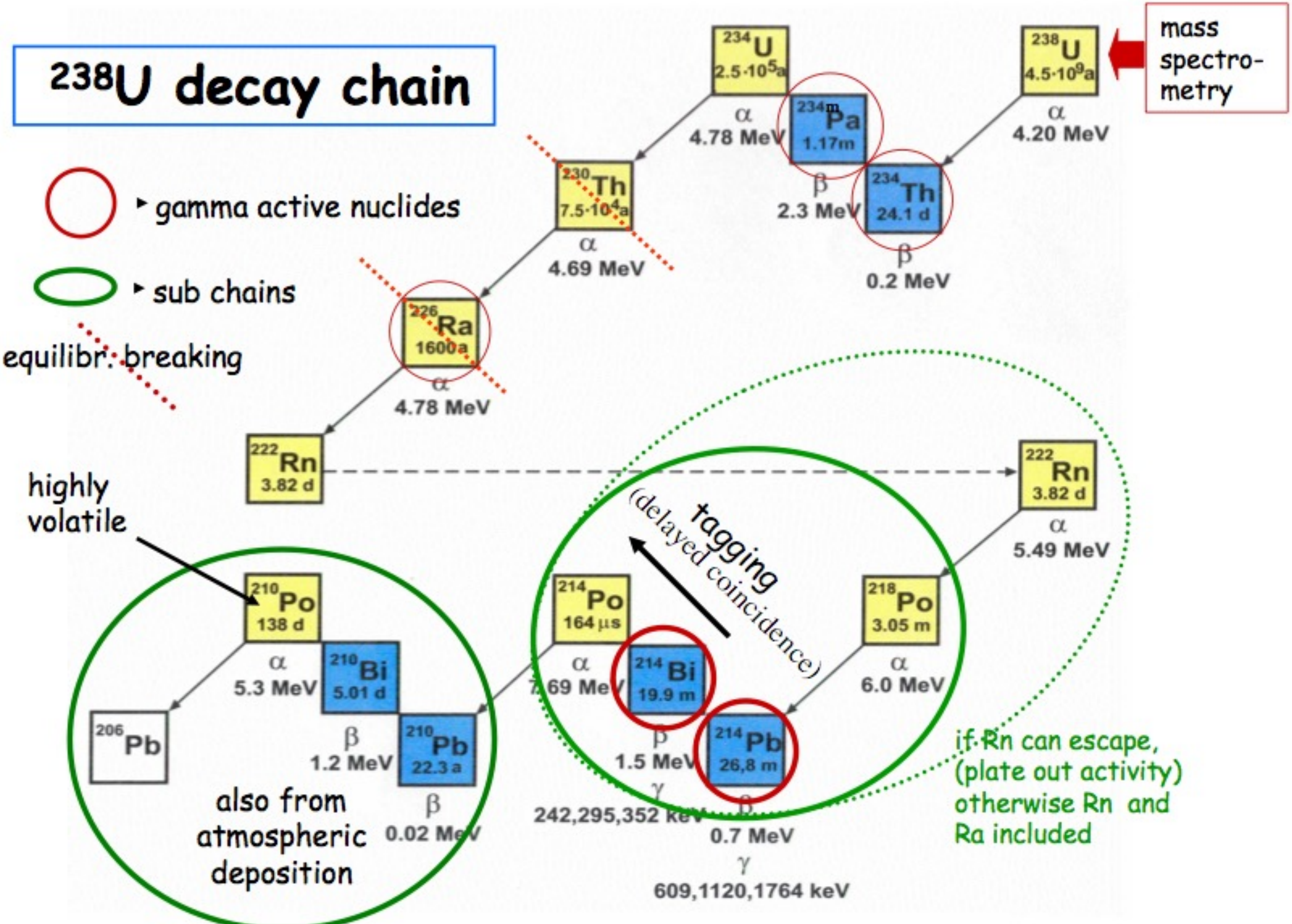
238U decay chain
gamma active nuclides
sub chains
equilibr. breaking
mass spectro-metry
234U 2.5·10^5a
238U 4.5·10^9a
α 4.78 MeV
234mPa 1.17m
α 4.20 MeV
230Th 7.5·10^4a
β 2.3 MeV
234Th 24.1 d
α 4.69 MeV
β 0.2 MeV
226Ra 1600a
α 4.78 MeV
222Rn 3.82 d
highly volatile
222Rn 3.82 d
α 5.49 MeV
tagging (delayed coincidence)
210Po 138 d
214Po 164 µs
218Po 3.05 m
α 5.3 MeV
210Bi 5.01 d
α 7.69 MeV
214Bi 19.9 m
α 6.0 MeV
206Pb
β 1.2 MeV
210Pb 22.3 a
β 1.5 MeV
214Pb 26,8 m
γ 242,295,352 keV
also from atmospheric deposition
β 0.02 MeV
β 0.7 MeV
γ 609,1120,1764 keV
if Rn can escape, (plate out activity) otherwise Rn and Ra included

^{232}Th decay chain

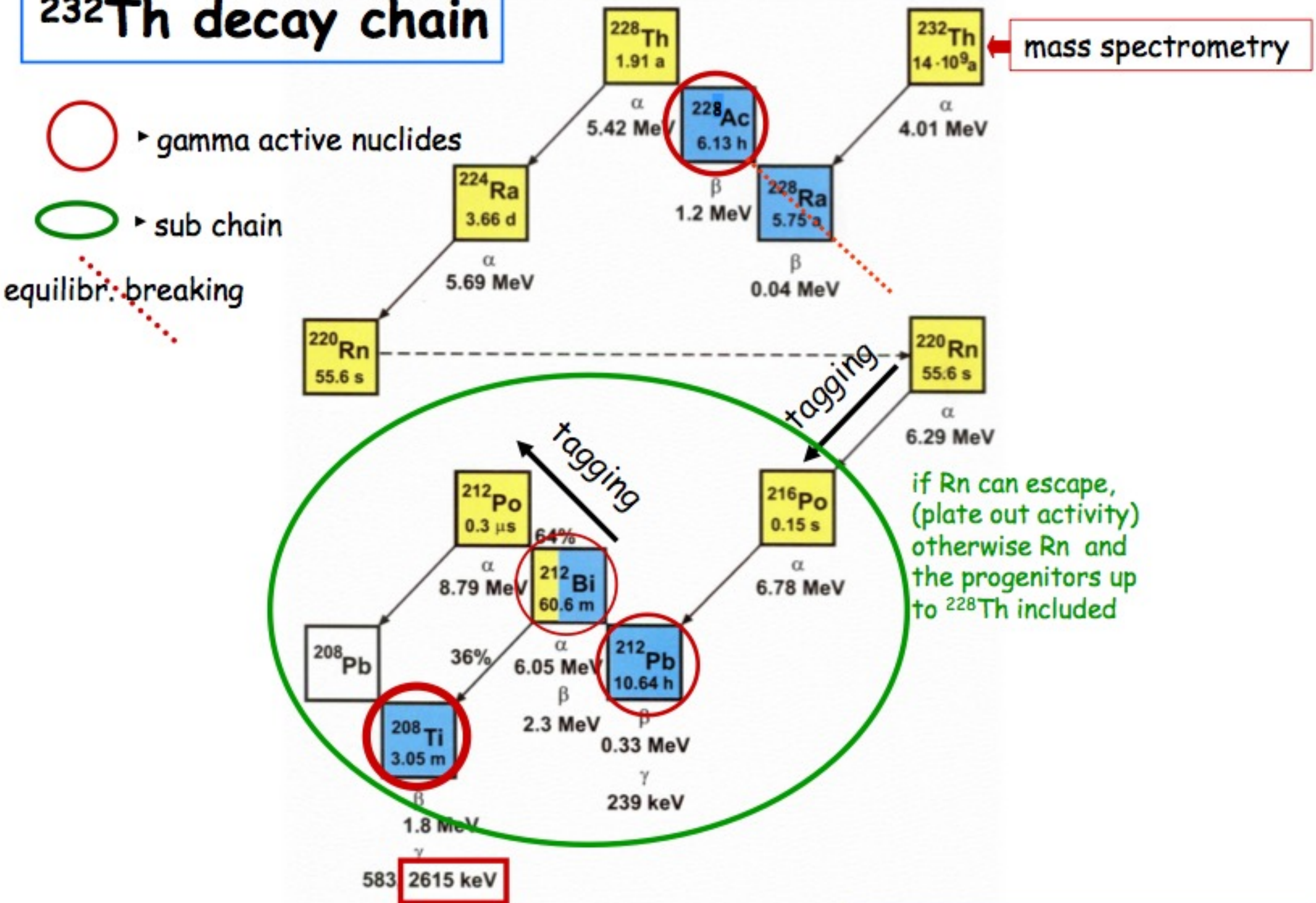

disequilibrium in natural decay chains

sample	activity of U/Th progenies [mBq/kg] and their ratios					
	^{234m}Pa	^{226}Ra	$^{234m}Pa/^{226}Ra$	^{228}Th	^{228}Ra	$^{228}Th/^{228}Ra$
WTS steel	121±18	0.99±0.15	122±26	3.7±0.4	1.7±0.2	2.18±0.35
pre WW1 steel	5.7±1.4	0.15±0.02	38±11	0.46±0.07	0.47±0.05	0.98±0.18

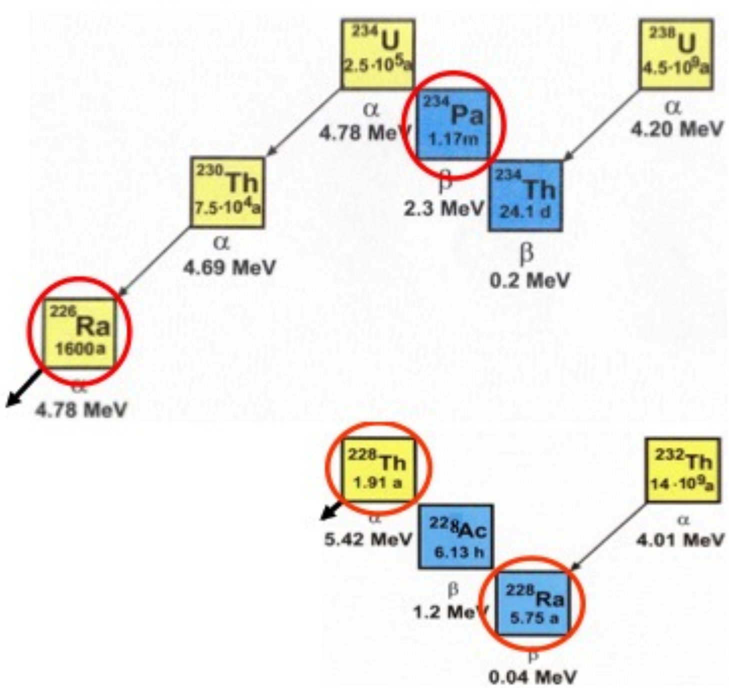

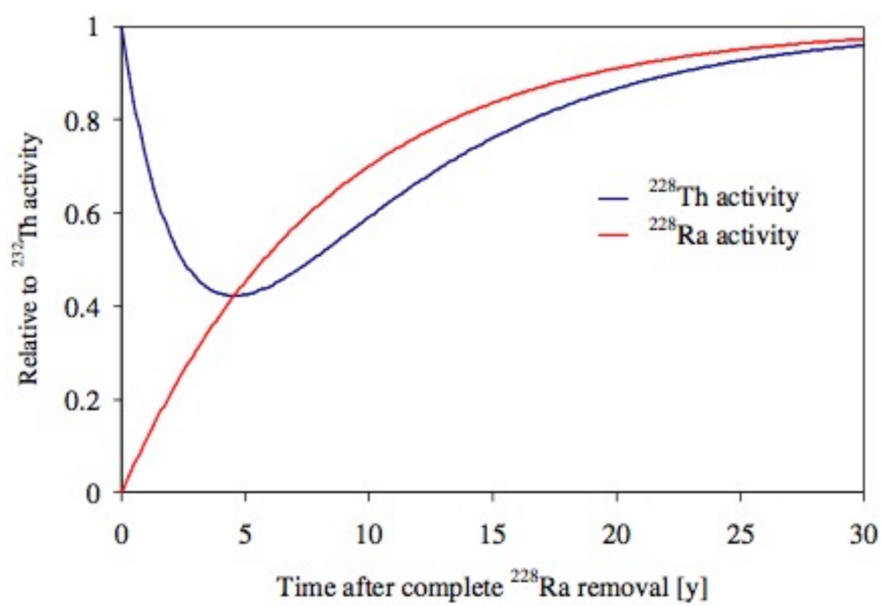

Rn and its progenies and other airborne radionuclides

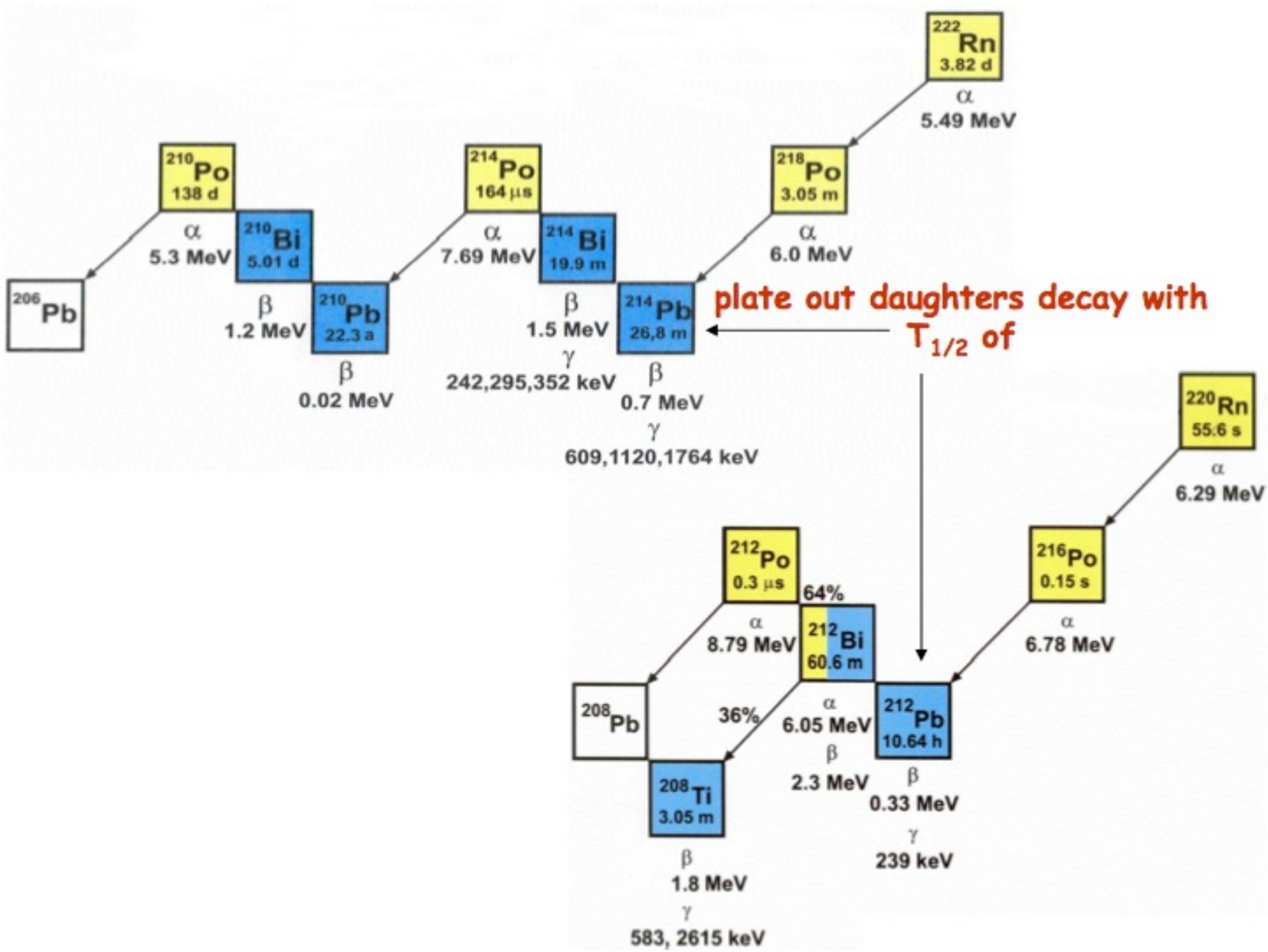

Rn and its progenies

$^{116}CdWO_4$ crystal scintillator in the DAMA Crys at **Gran Sasso Lab** Lab

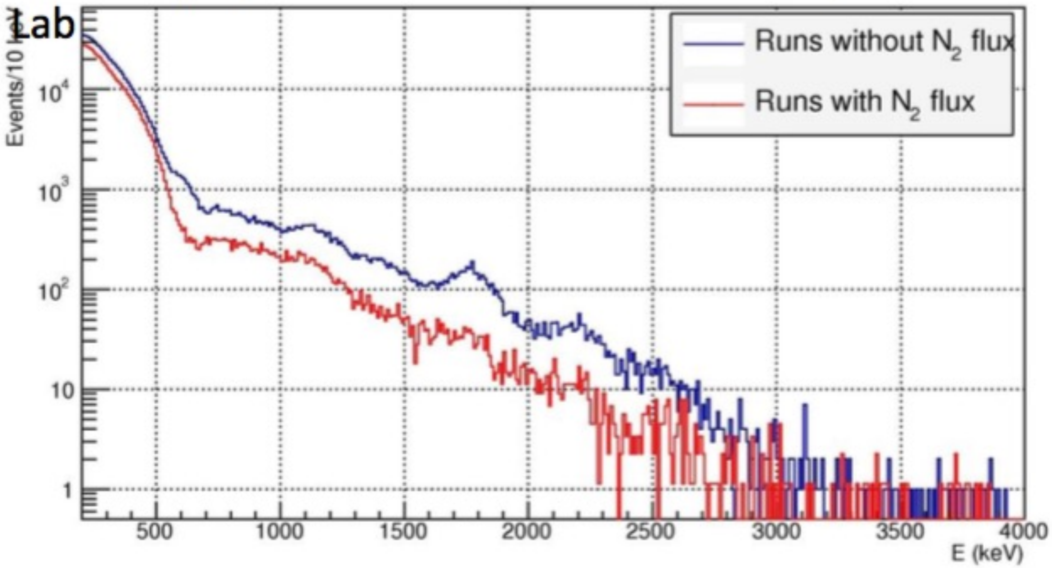

Rn in Borexino

^{210}Po (daughter of ^{210}Pb) appear in Borexino as result of Radon penetration / emanation

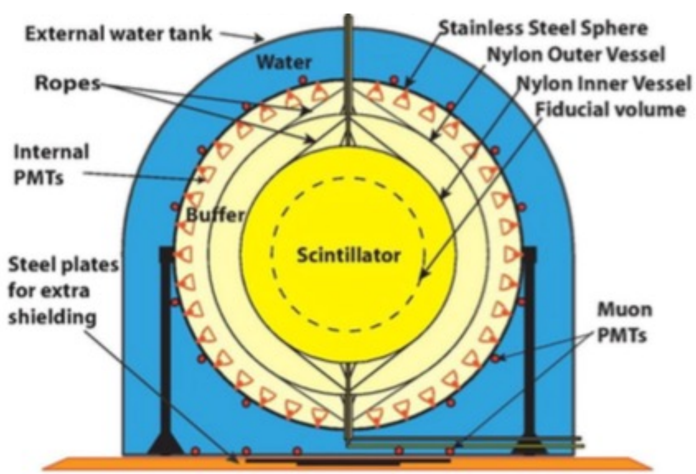

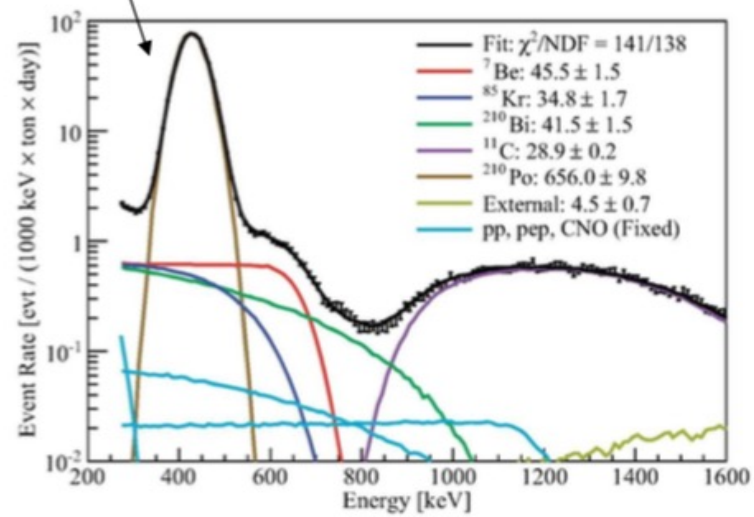

Suppression of background

3) External shielding:

- against γ - Pb, Cu, Fe (20-50 cm)
- against neutrons - polyethylene (borated, lithium dopped)

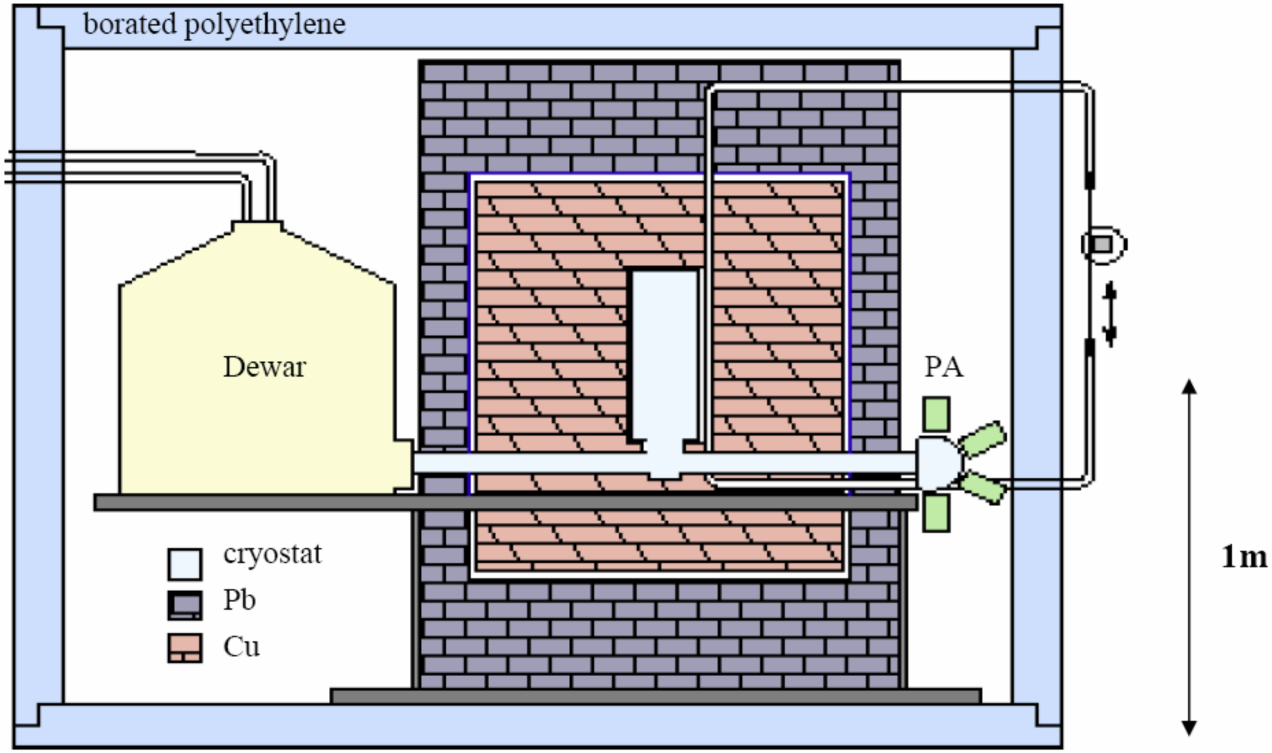

Measurement of lead with GeMPI

lead sample	weight	time	specific activity [µBq/kg]				
	[kg]	[d]	^{226}Ra	^{228}Th	^{40}K	^{207}Bi	^{210}Pb
DowRun	144.6	101.7	< 29	< 22	440 ± 140	98 ± 24	$(2.7 \pm 0.4) \times 10^7$
Boliden	144.3	75.0	< 46	< 31	460 ± 170	< 13	$(2.3 \pm 0.4) \times 10^7$
roman	22.1	37.2	< 45	< 72	< 270	< 19	$< 1.3 \times 10^6$
	bolometric measurement: Allesandrello et al. NIM B142 (1998) 163						$< 4 \times 10^3$

DAMA R&D passive shield

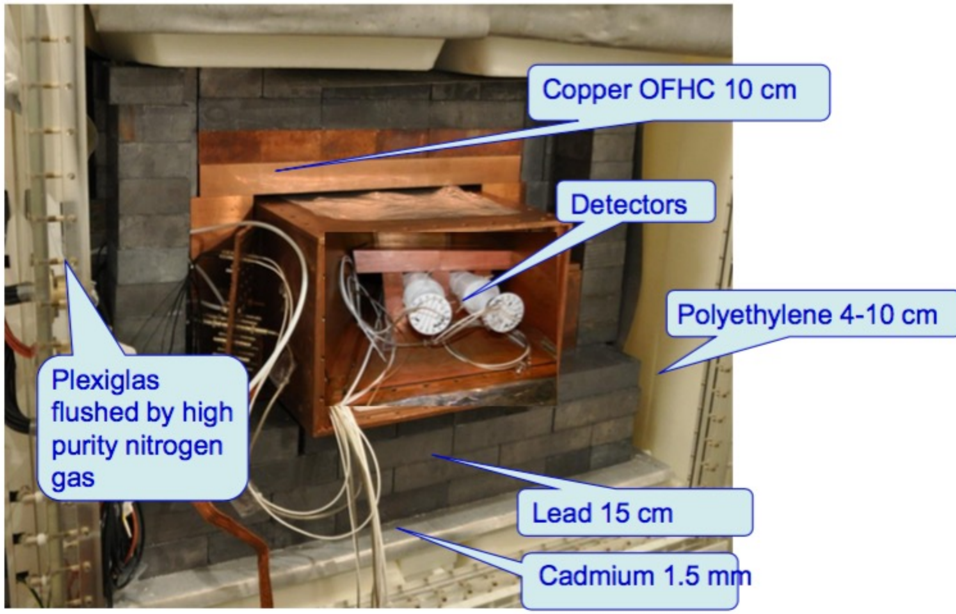

Passive shield typically is made of a few layers to shield against gamma and neutrons, sealing from radon, and to minimize cost

- **Combination of different materials in passive shield is reasonable to minimize cost (e.g. OFHC is more expensive than that lead), and to provide shield both from γs and neutrons**
- **One should foreseen possibilities for calibration by radioactive sources**

Some examples of shields (passive shield)

Solotvina experiment: passive shield

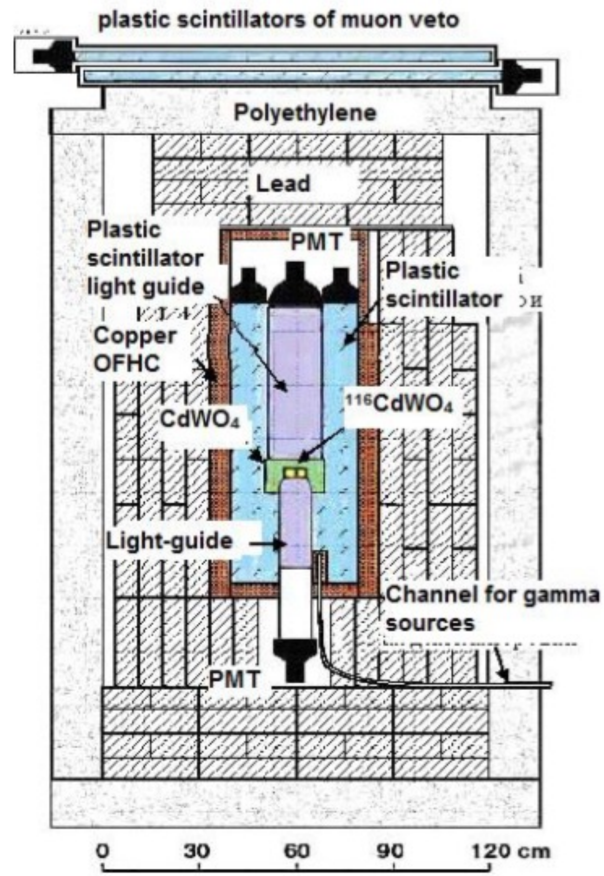

Phys. Rev. C 68 (2003) 035501

Water shield in Borexino

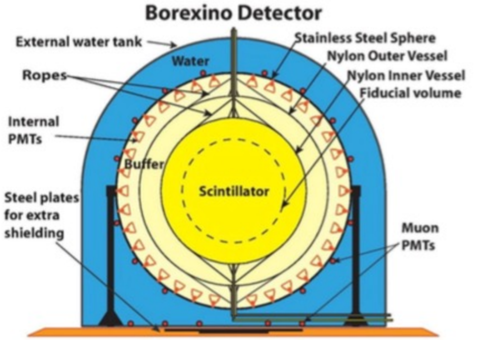

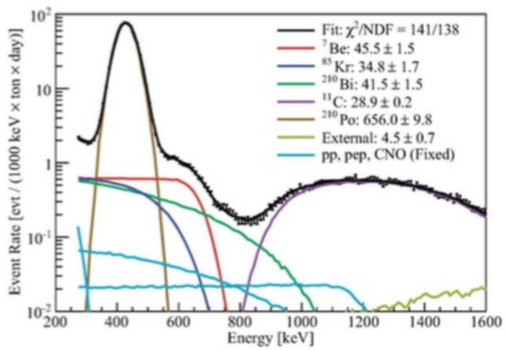

Water can be deeply purified by complex approach (e.g. in Borexino):

- filtering (0.1 μm)
- Osmosis unit
- De-ionization
- Current flow of high purity nitrogen in a stripping column

Water is unavoidable for very large set-ups due to high cost of metals

Some examples of shields (active shields)

- **The external layer of the detector serves as an active shield**
- **Outer water Cherenkov detector (cosmic muons veto)**

SNO (Sudbury Neutrino Observatory)

heavy water Cherenkov detector to measure solar neutrino (ν_e, ν_μ, ν_τ)

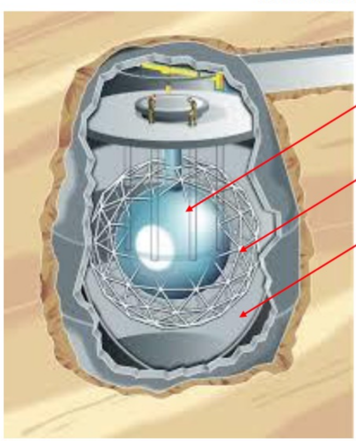

Acrylic vessel with 10^3 ton of heavy water

Support construction for ~10^4 PMTs

Outer vessel filled with light water as passive shield

GERDA water shield

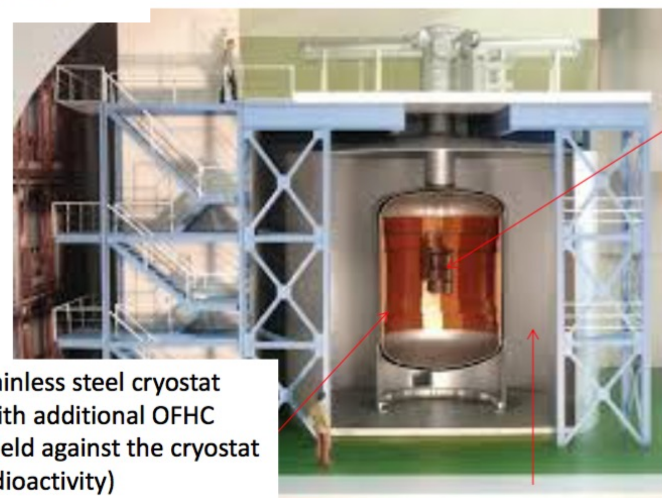

Bare HPGe detectors ^{76}Ge

Stainless steel cryostat (with additional OFHC shield against the cryostat radioactivity)

Ultra-pure water passive shield, acts also as active Cherenkov muon veto

Question: for what reason bare detectors were chosen?

Active shield (veto)

- Plastic scintillators
- Liquid scintillators
- Inorganic scintillators (NaI(Tl), CsI(Tl), BGO, $CdWO_4$)
- Cherenkov counter

Use of Fiducial Volume (FV)

1. The volume used to make physics measurements
2. The volume where the detector is assumed to be well understood
3. For our purpose: the volume where the background is reduced

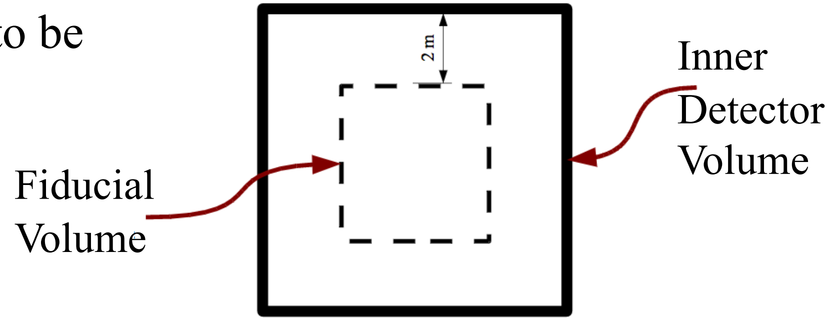

Fiducial Volume

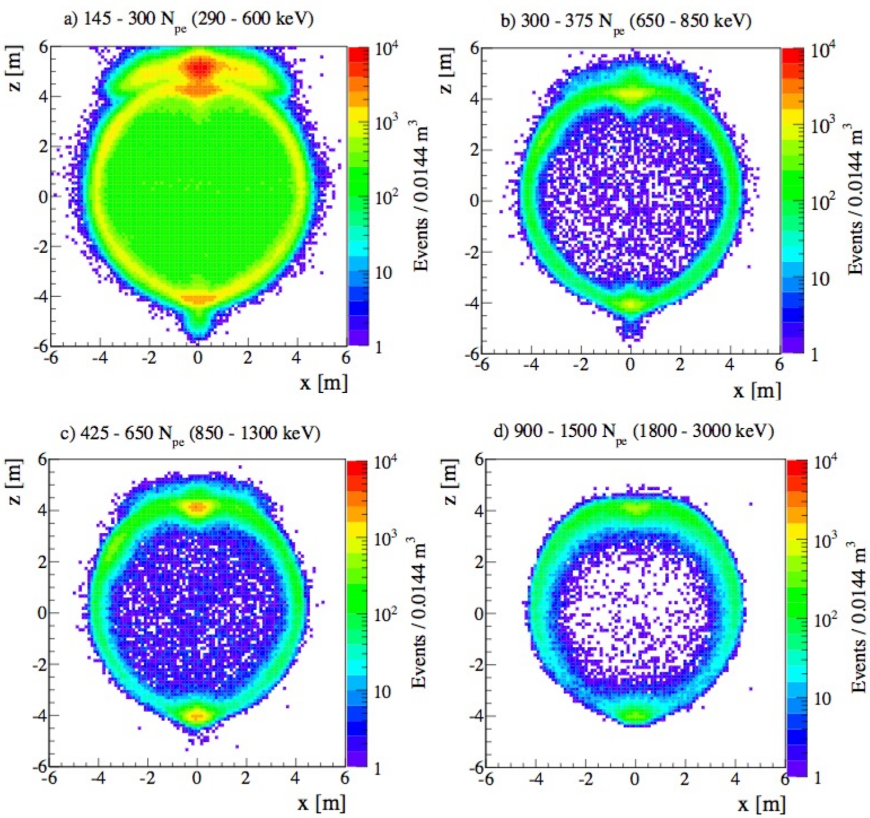

The case of Borexino

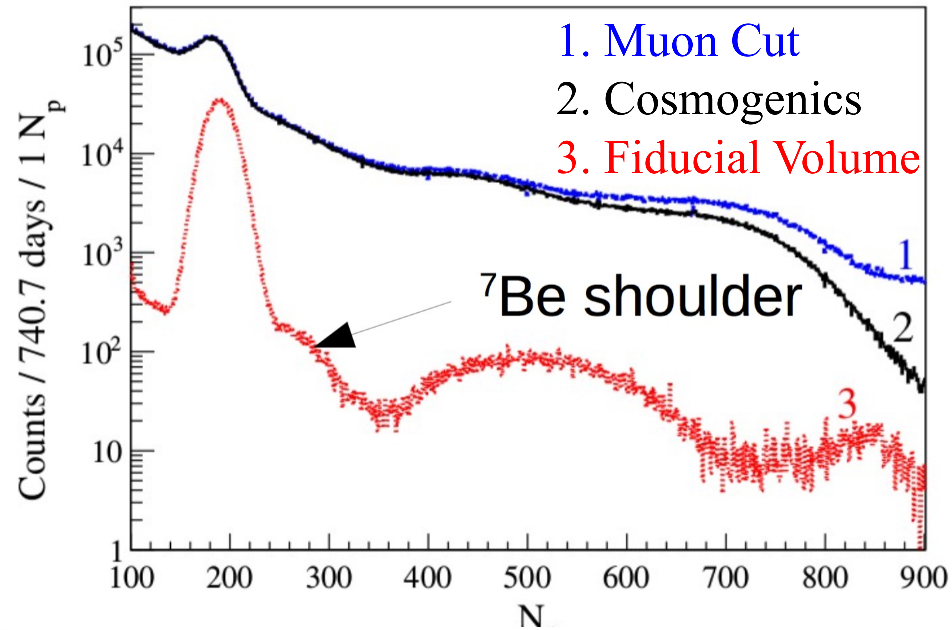

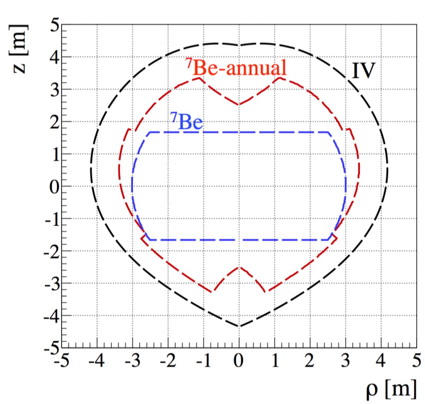

- The choice of the FV is related to the effect searched for
- Trade-off between high exposure and low bckg

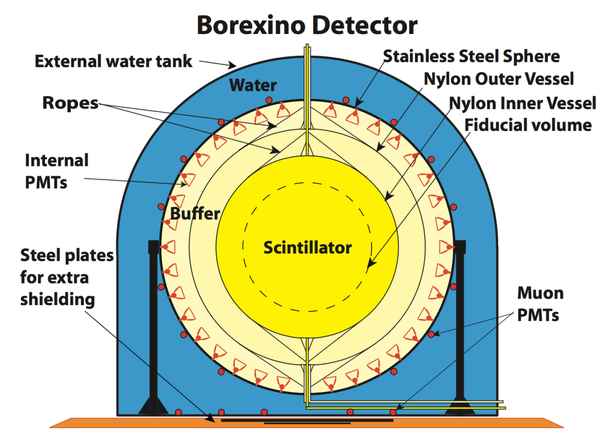

Fiducial Volume

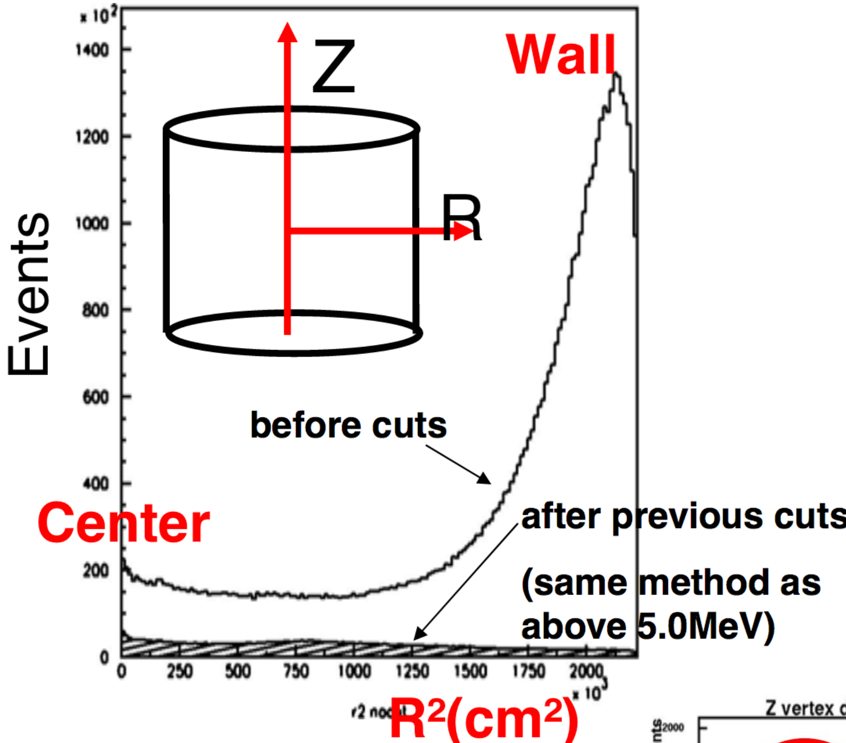

The case of SuperKamiokande

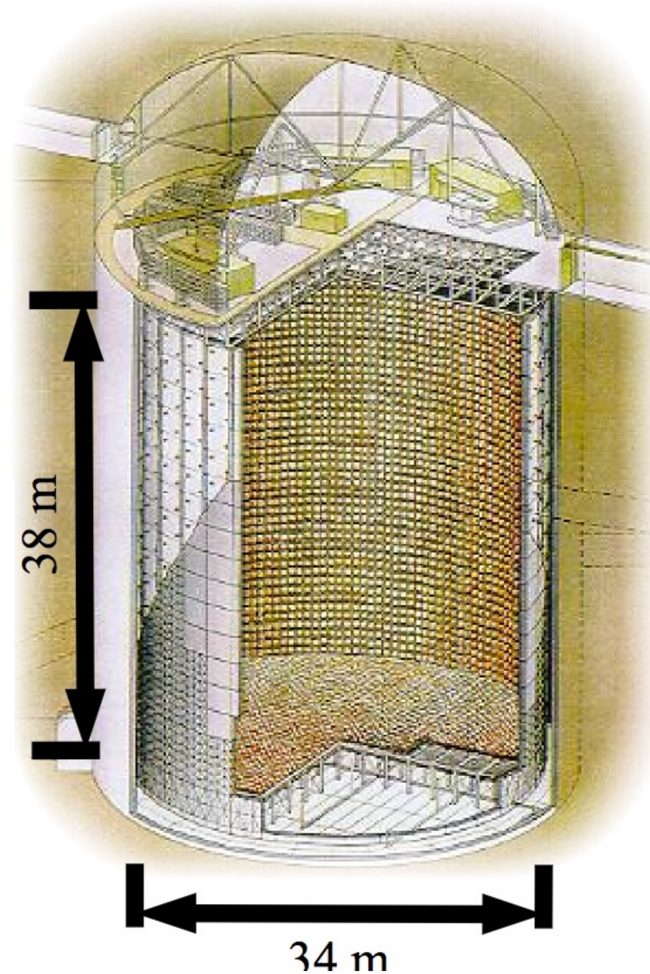

- Analysis of lower energy region in SK-I
- Vertex position distribution of background (4.5 – 5.0 MeV)
- Tighter cuts to reduce external bckg
- Improved vertex reconstruction program.
- Remove high radon periods.

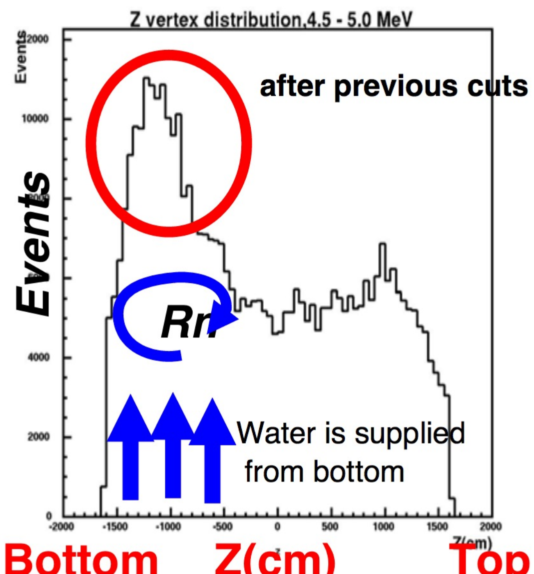

Coincidence techniques

Reduction of internal ^{208}Tl and ^{214}Bi

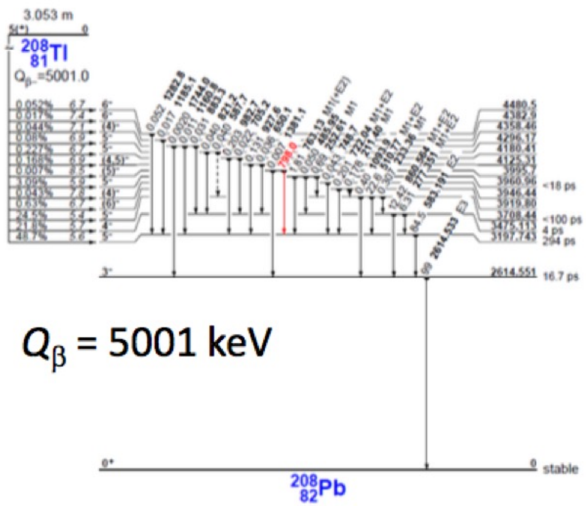

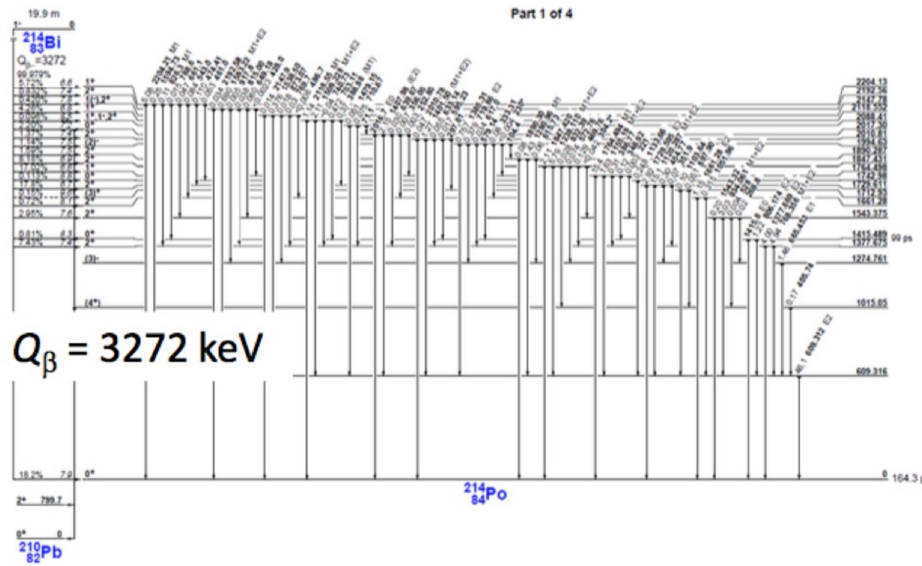

Anticoincidence can reduce background by factor 2-10 (depending on 1) energy threshold, 2) presence of passive materials between detectors, 3) multiplicity of the set-up

Coincidence techniques

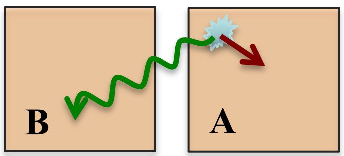

residual ^{nat}K

^{40}K: **$\delta = 0.0117\ \%$**

$T_{1/2} = 1.248 \times 10^9$ yr (EC = 10.86%; $\beta^- = 89.14\ \%$)

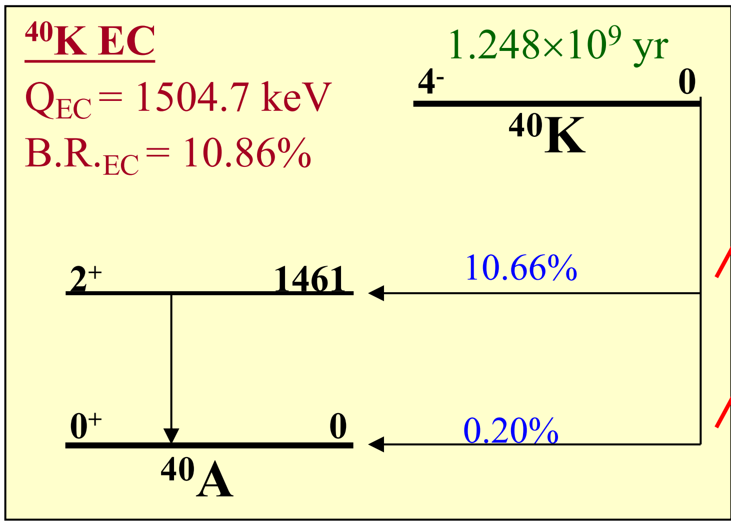

$$\Rightarrow 1\text{ppb}\ ^{nat}K: \quad a(^{40}K) = \frac{1000 \cdot 10^{-9} \cdot N_A}{39.1}\ \delta\ \frac{\ln 2}{T_{1/2}} = 31.7\ \mu\text{Bq/kg}$$

L1461: **$EC_K = 76.3\%$; $EC_L = 20.9\%$; $EC_{M+} = 2.74\%$**

L0: **$EC_K = 87.9\%$; $EC_L = 8.6\%$; $EC_{M+} = 1.26\%$**

The 1461 keV γ can escape from one detector (*A*) and hit another one causing a double coincidence. X-rays/Auger electrons give rise in *A* to a 3.2 keV peak

r

The probability for ^{40}K EC from shell K to the 1461 keV level of ^{40}Ar is: $P_{40K\ EK \rightarrow 1461} = 10.66\% \times 76.3\% = 8.1\%$ in such a case a 1461 keV γ is emitted together with the 3.2 keV X-rays/Auger electrons from shell K of ^{40}Ar (this last is contained in the detector with efficiency ~ 1)

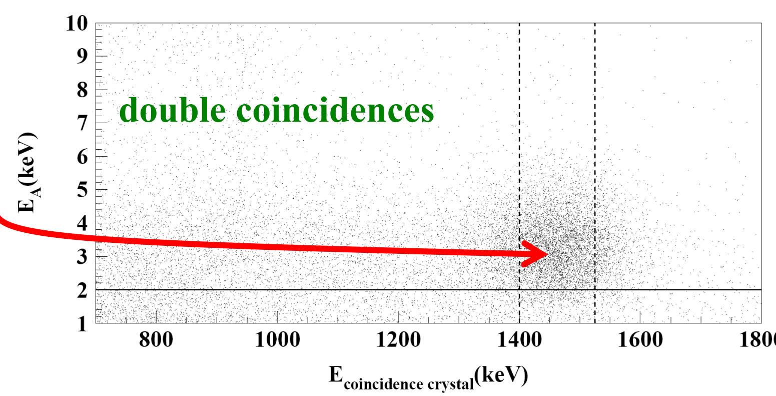

The 3.2 keV peak offers also the proof of the physical threshold of the detectors and an intrinsic calibration for each one in the lowest energy region

Coincidence techniques

The case of cosmogenic in-situ ^{11}C in Borexino

Three-Fold-Coincidence

$$\mu(+\text{ secondaries}) + {}^{12}C \rightarrow \mu\ (+\text{ secondaries}) + {}^{11}C + n.$$

Triple coincidence among:

1. The muon
2. The neutron capture by H
3. The ^{11}C decay

^{11}C β^{+} decays with a mean life of 29.4 min and an end-point energy of 0.96 MeV

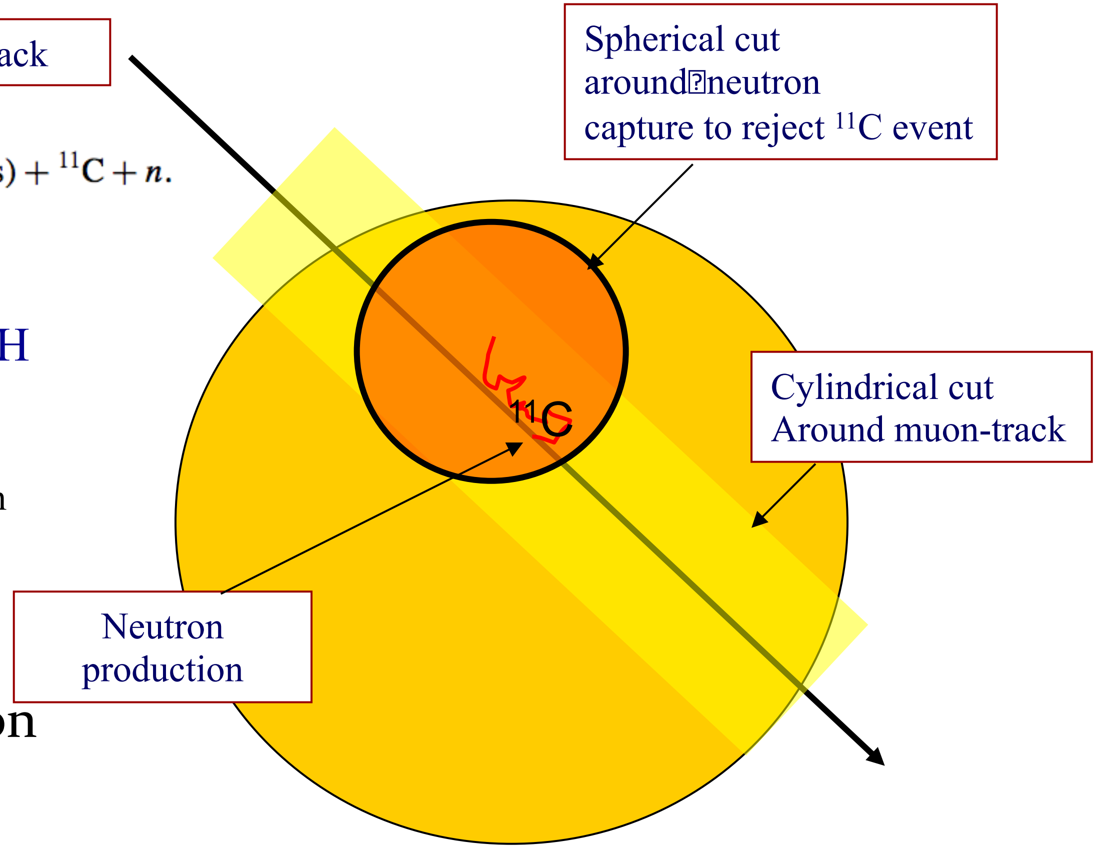

Muons crossing the LS produce at least one neutron in 95% of cases

Goal: reduce ^{11}C background

Borexino coll: CNO and pep neutrino spectroscopy in Borexino: measurement of the deep-underground production of cosmogenic ^{11}C in an organic liquid scintillator, **Phys. Rev. C 74, 045805 (2006).**

TFC decreases 11C rate to ~10% of its original value with ~50% loss of exposure.

Limiting background internal ^{210}Bi.

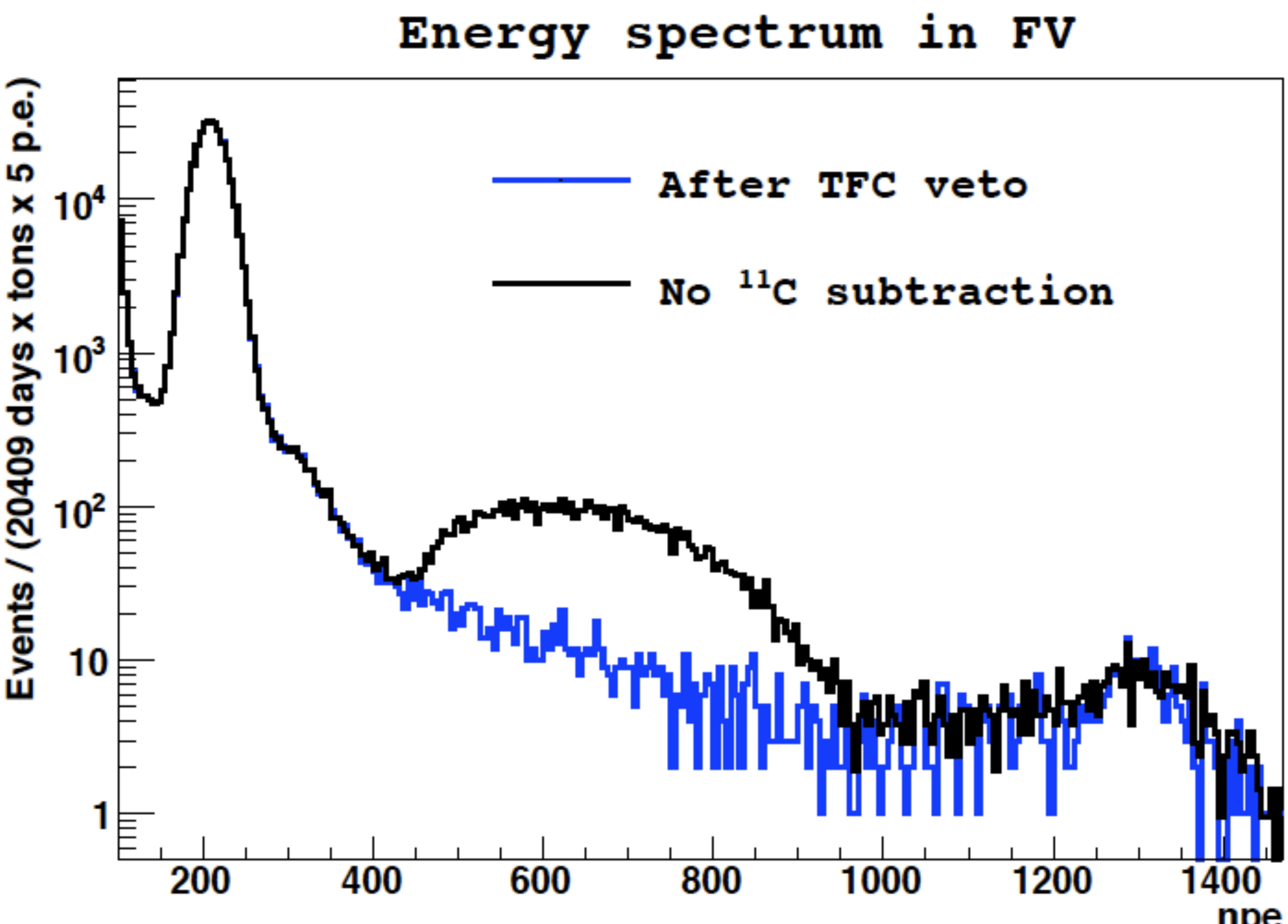

Pulse Shape Discrimination (PSD)

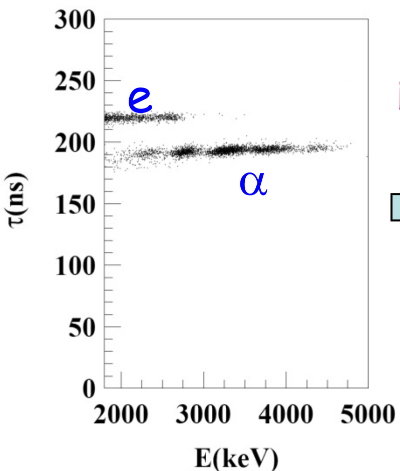

α/e pulse shape discrimination has practically 100% effectiveness in the MeV range

The measured α yield in the new DAMA/LIBRA detectors ranges from 7 to some tens α/kg/day

^{238}U residual contamination in NaI(Tl) of DAMA/LIBRA

$$\tau = \frac{\int t \cdot f(t) \mathrm{d}t}{\int f(t) \mathrm{d}t} \approx \frac{\sum_i h_i t_i}{\sum_i h_i}$$

First estimate: considering the measured α and ^{232}Th activity, if ^{238}U chain at equilibrium $\Rightarrow$ ^{238}U contents in new detectors typically range from 0.7 to 10 ppt

But, hypothesis of equilibrium is not confirmed by the study of the α particles energy distributions:

Example: 5 α peaks

1. ^{232}Th(Q_α=4.08 MeV) + ^{238}U(4.27 MeV)
2. ^{234}U(4.86 MeV) + ^{230}Th(4.77 MeV) + ^{226}Ra(4.87 MeV)
3. ^{210}Po(5.41 MeV) + ^{228}Th(5.52 MeV) + ^{222}Rn(5.59 MeV) + ^{224}Ra(5.79 MeV)
4. ^{218}Po(6.12 MeV) + ^{212}Bi(6.21 MeV) + ^{220}Rn(6.41 MeV)
5. ^{216}Po(6.91MeV)

live time = 570 h

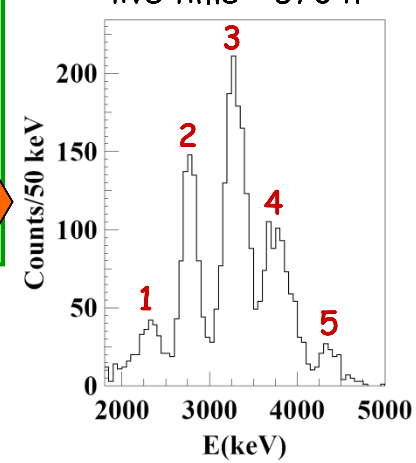

^{238}U chain splitted into 5 subchains: $^{238}U \rightarrow {}^{234}U \rightarrow {}^{230}Th \rightarrow {}^{226}Ra \rightarrow {}^{210}Pb \rightarrow {}^{206}Pb$

Thus, in this case: (2.1±0.1) ppt of ^{232}Th; (0.35 ±0.06) ppt for ^{238}U

and: (15.8±1.6) μBq/kg for ^{234}U + ^{230}Th subchain; (21.7±1.1) μBq/kg for ^{226}Ra subchain; (24.2±1.6) μBq/kg for ^{210}Pb subchain.

Time Amplitude Analysis

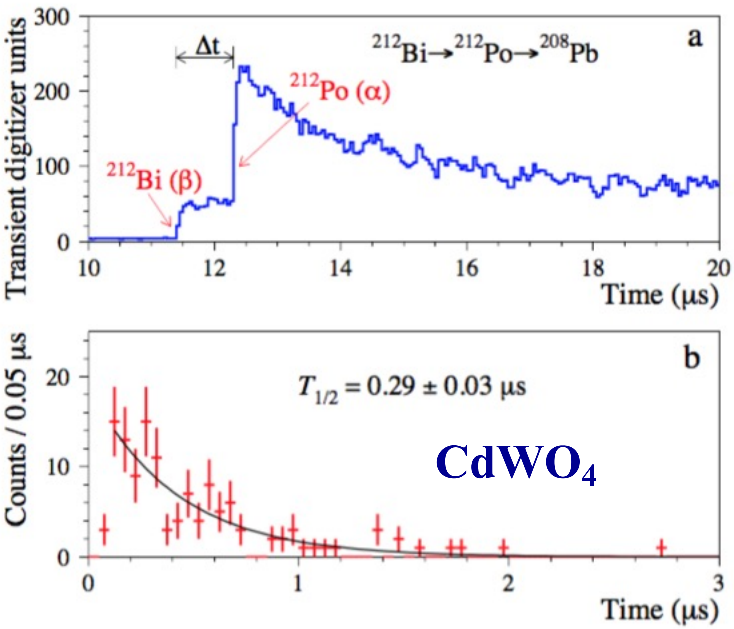

Bi-Po events

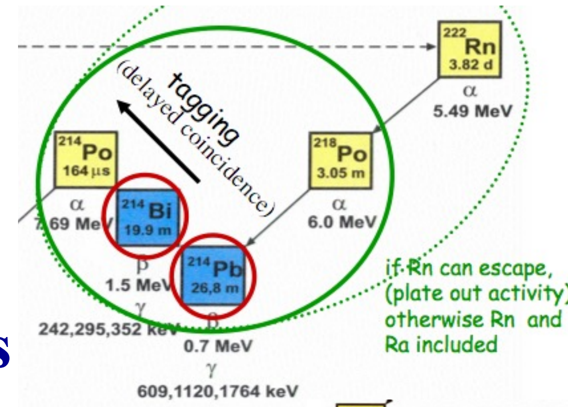

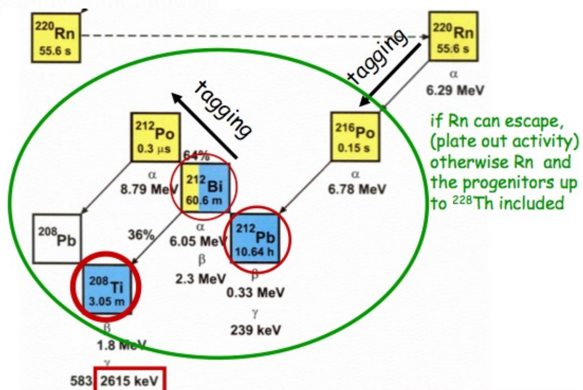

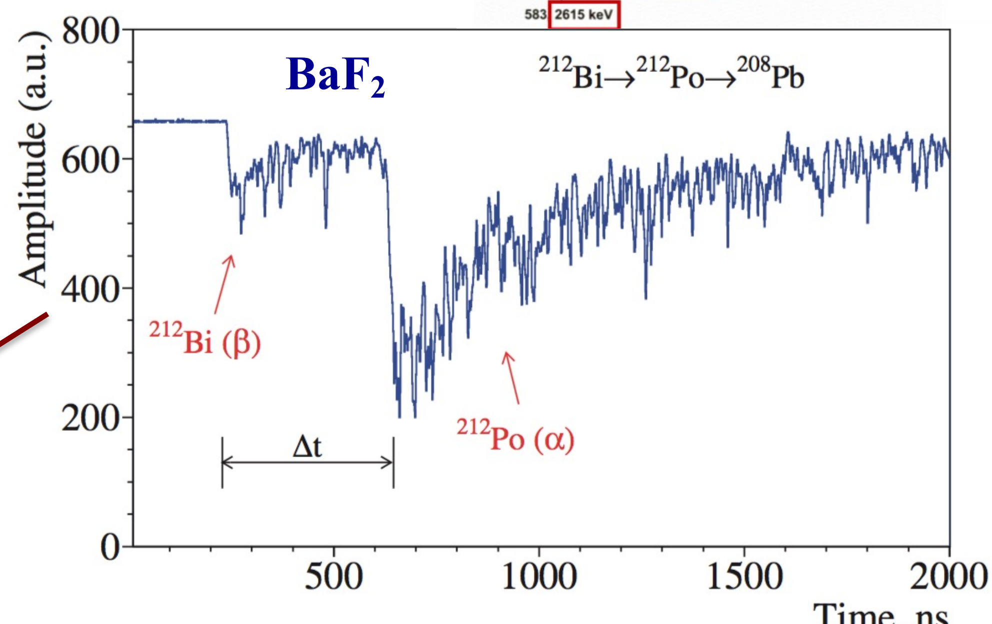

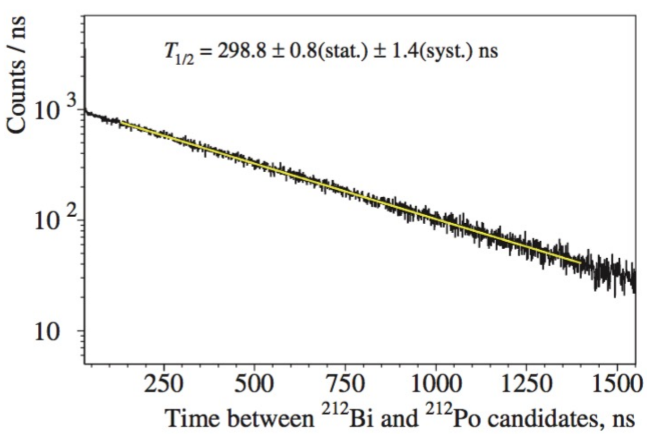

^{212}Bi-^{212}Po in ^{116}CdWO$_4$

$$^{212}\mathrm{Bi} \xrightarrow{\beta} {}^{212}\mathrm{Po} \xrightarrow{\alpha} {}^{208}\mathrm{Pb}$$

$T_{1/2}$= 0.3 μs

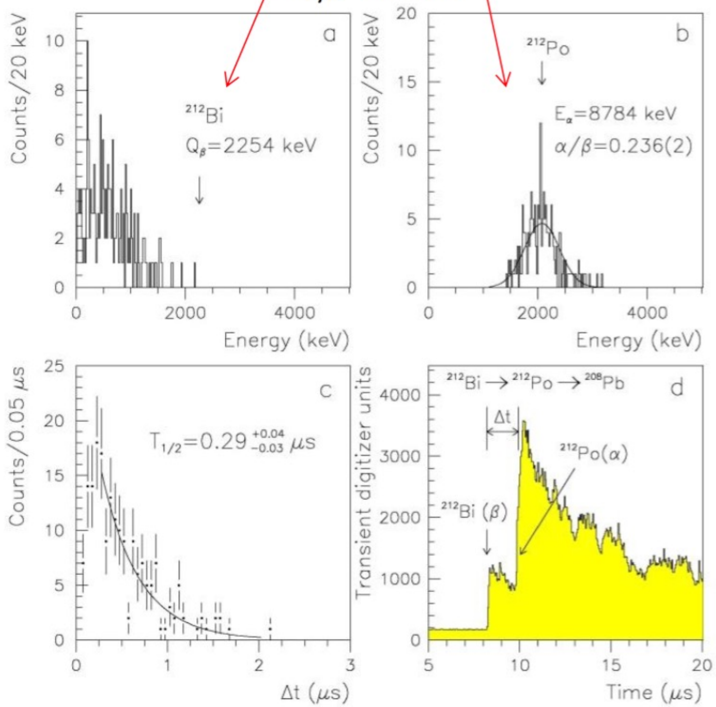

^{214}Bi-^{214}Po in ^{116}CdWO$_4$

$$^{214}\mathrm{Bi} \xrightarrow{\beta} {}^{214}\mathrm{Po} \xrightarrow{\alpha} {}^{210}\mathrm{Pb}$$

$T_{1/2}$= 164 μs

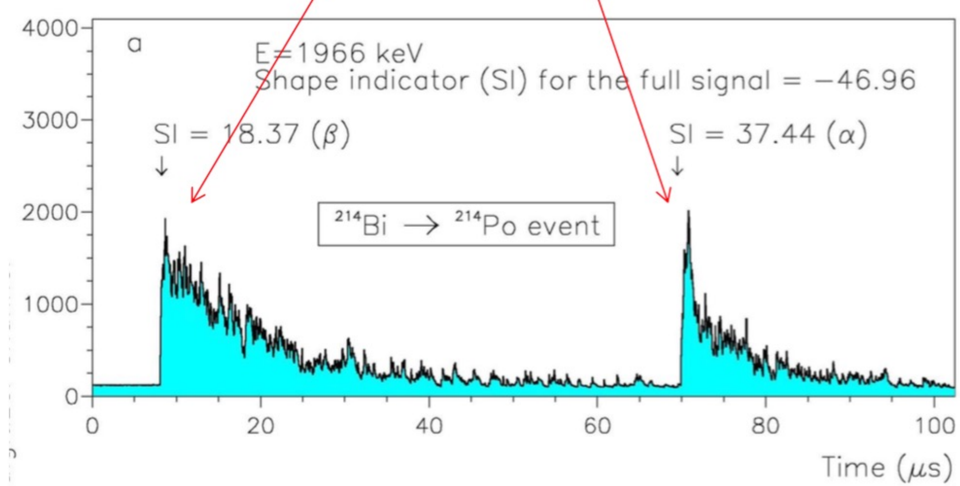

Summary

- Surface contamination is rather dangerous source of background
- Pulse-shape and time-amplitude analyses are powerful approaches to analyze internal radioactive contamination of detectors
- Noise can be rejected by pulse-shape discrimination, stability (time and energy) should be checked
- Monte Carlo simulation is a useful tool to analyze background spectra (learn GEANT4, EGS4, etc)
- Crystal scintillators are detectors with rather wide range of radioactive contamination (13 orders of magnitude). Composition and chemical properties are the most crucial issues
- Deep purification of materials is strongly requested by low counting experiments: crystallization in aqueous solutions, distillation, zone melting, recrystallization

Direct detection experiments

The direct detection experiments can be classified in **two classes**, depending on what they are based:

1. on the recognition of the signals due to Dark Matter particles with respect to the background by using a ***model-independent* signature**
2. on the use of uncertain techniques of statistical **subtractions** of the e.m. component **of the counting rate** (adding systematical effects and lost of candidates with pure electromagnetic productions)

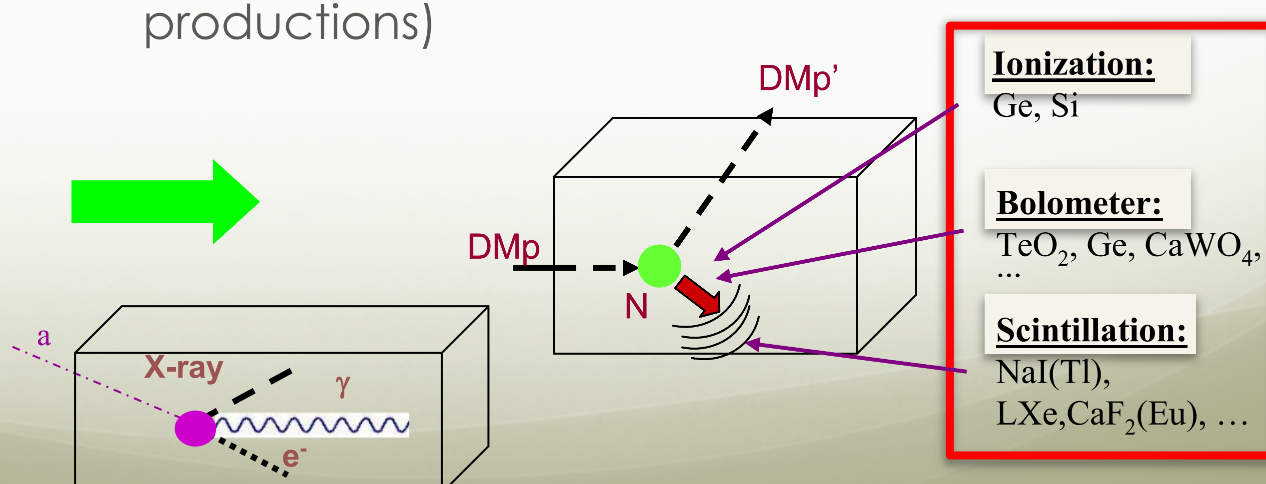

Direct detection experiments

Summarizing, the detectors for DM:

- must have very low-energy thresholds (order of keV at least)
- must have very low intrinsic bckg
- must be well shielded by external environmental radiation (muons, neutrons, gammas, ...)
- must be stable with time
- must have very good experimental features (energy resolution, check of the energy scale, uniformity of the detector, and many others)

Many techniques/experiments on the market:

- Scintillation detectors: NaI(TI) ...
- Liquid noble gases: LXe, LAr, LNe
- Bolometers (heat vs ionization): Ge, Si
- Bolometers (heat vs scintillation): $CaWO_4$
- Ionization detectors: Ge
- and others…

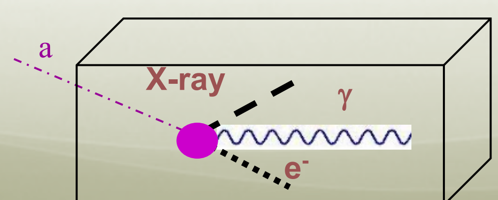

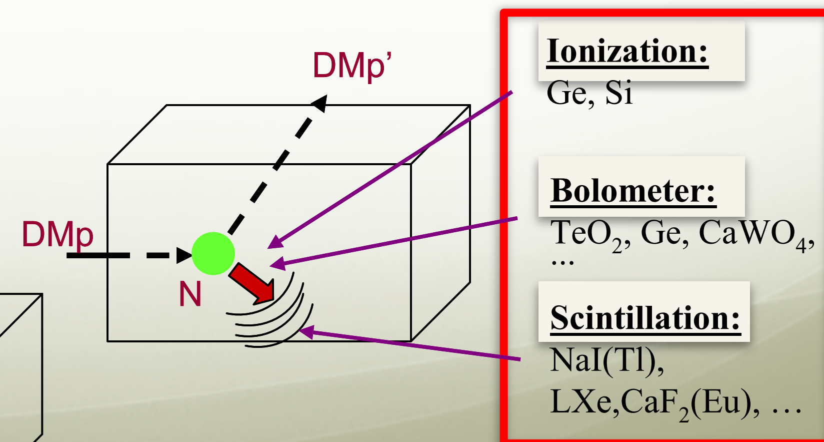

Experiments using liquid noble gases

PSD in single phase detector:

- pulse shape discrimination γ/recoils from the UV scintillation photons

DAMA/LXe

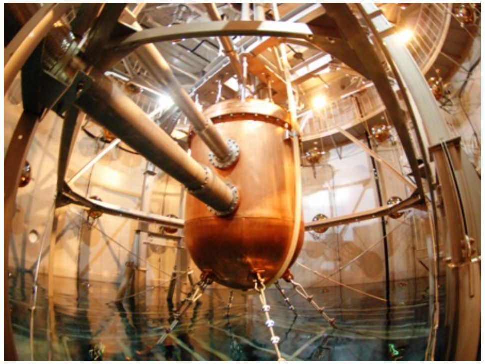

XMASS

in dual phase detector:

- prompt signal (S1): UV photons from excitation and ionization
- delayed signal (S2): e^- drifted into gas phase and secondary scintillation due to ionization in electric field

Statistical rejection of e.m. component of the counting rate

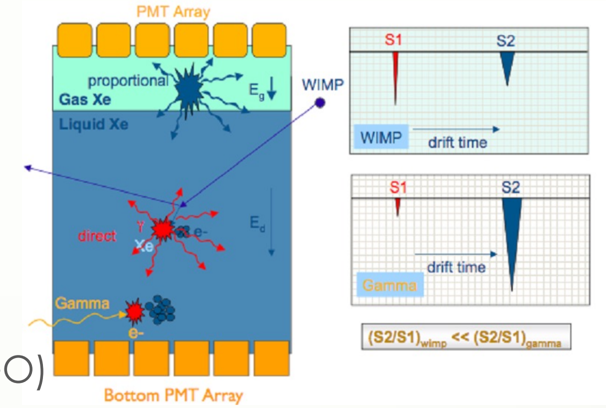

WARP, XENON10, -100, -1T, -nT, LUX, PANDAX, DarkSide-50, DEAP-3600, CLEAN, ArDM ➔ towards larger target masses (LZ, Darwin, DS-20k, ARGO)

- **Non-uniform** response of detector: intrinsic limit
- **UV light**, **unlinearity** (more in larger volumes)
- **Correction** procedures applied; **Systematics**
- Physical **energy threshold not robust**
- Poor energy **resolution**
- **Light responses** for electrons and recoils at low energy
- **Quenching factors** measured with a much-more-performing detector **cannot be used** straightforward
- Etc.

Many cuts applied, each of them can introduce systematics. The systematics can be variable along the data taking period; can they and the related efficiencies be suitably evaluated in short period calibration?

After many cuts few events survive: intrinsic limit reached?

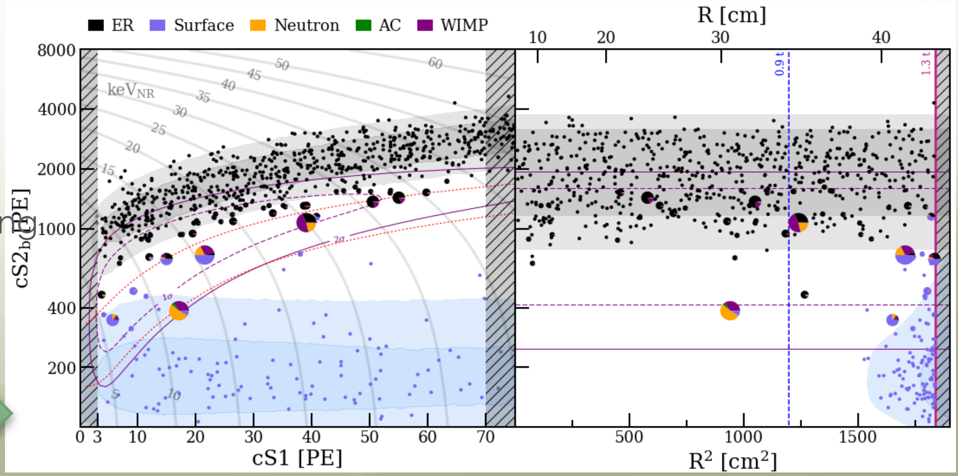

LAr at LNGS: DarkSide

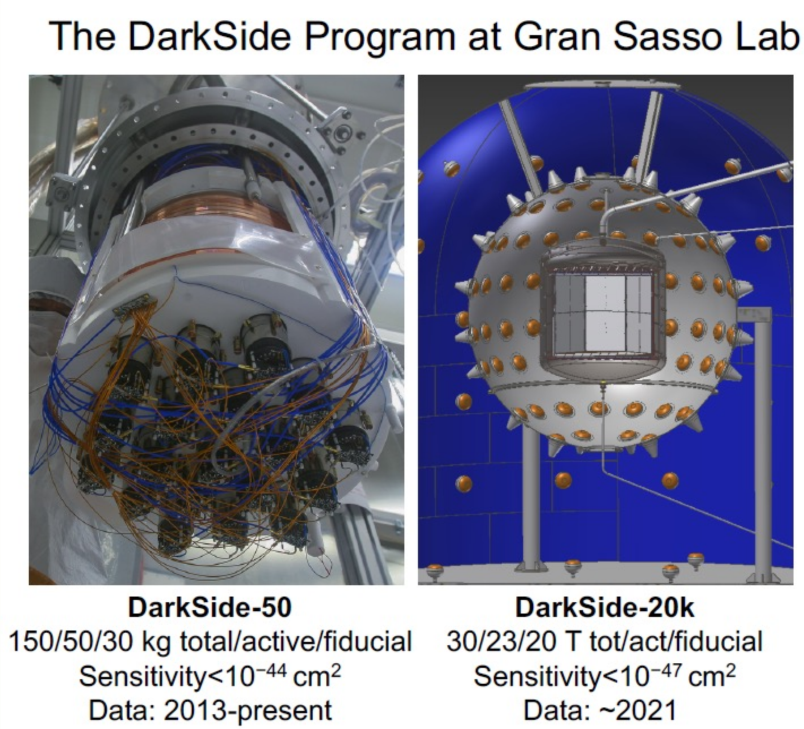

...toward DarkSide-20k

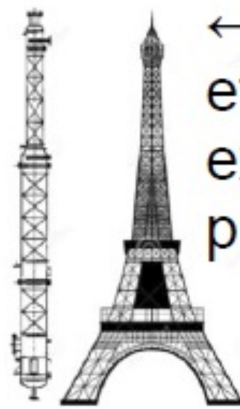

← Massive effort to extract and purify UAr

SiPMs replace → PMTs

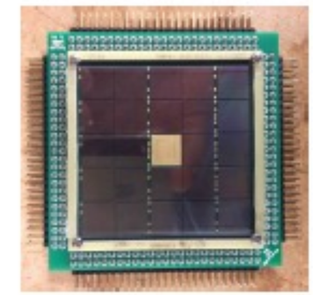

DarkSide

- Operated DarkSide-10 prototype for 1 year
- Constructed as part of DarkSide-50:
  - 1000 tonnes water Cherenkov muon veto
  - 30 tonnes organic liquid scintillator neutron veto
  - two Rn-free clean rooms for final preparation of the detector
  - argon recirculation, purification, and recovery systems
- All facilities built sized to house DarkSide-G2

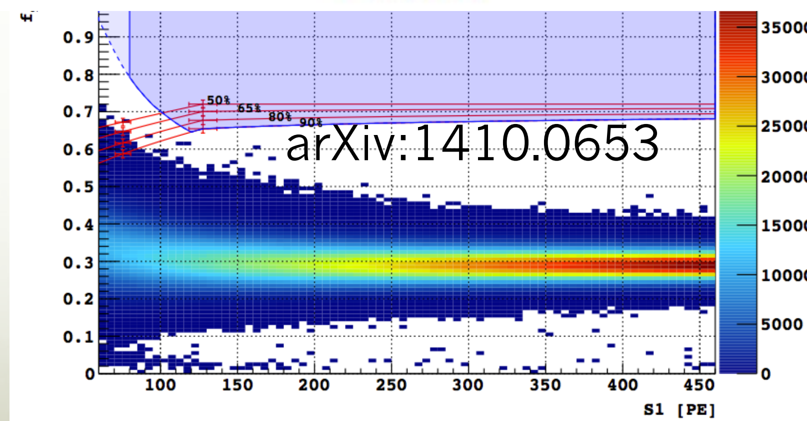

Technical comments similar as for XENON are expected (see above)

Double read-out bolometric technique
(ionization vs heat)

$$\Delta T = \frac{Q}{C_V}$$

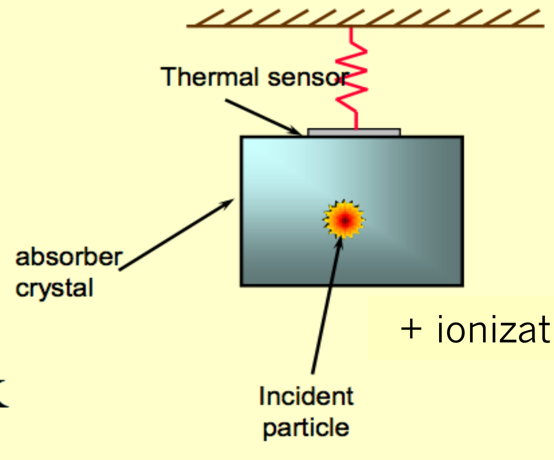

+ ionization

$$C_V = 1944 \frac{V}{V_m} \left(\frac{T}{\Theta}\right)^3 \text{ J/K}$$

Energy resolution <1 eV ~2eV @ 6 keV
~10 eV ~keV @ 2 MeV

Doped Semiconductors

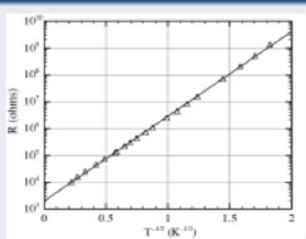

- α negative; $|\alpha| < 10$
- Resistance large
- Current bias and read voltage

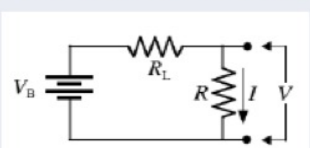

Superconducting transition-edge

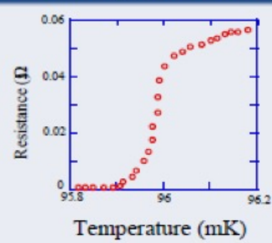

- α positive; $10 < \alpha < 1000$
- Resistance small
- Voltage bias and read current

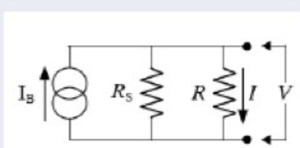

Double read-out bolometric technique
(ionization vs heat)

ZIP Detectors: Charge

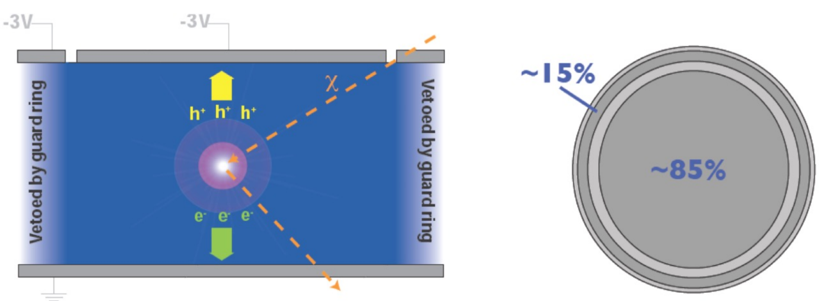

Inner Channel: ionization measurement
Outer Channel: fiducial volume

ZIP Detectors: Phonons

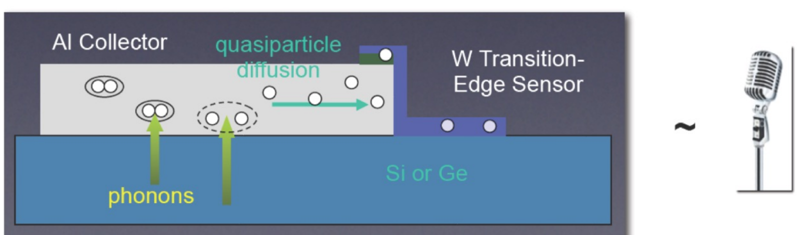

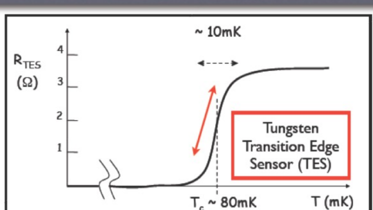

4 SQUID readout channels, each reads out 1036 TESs in parallel

CDMS: detection principle and response

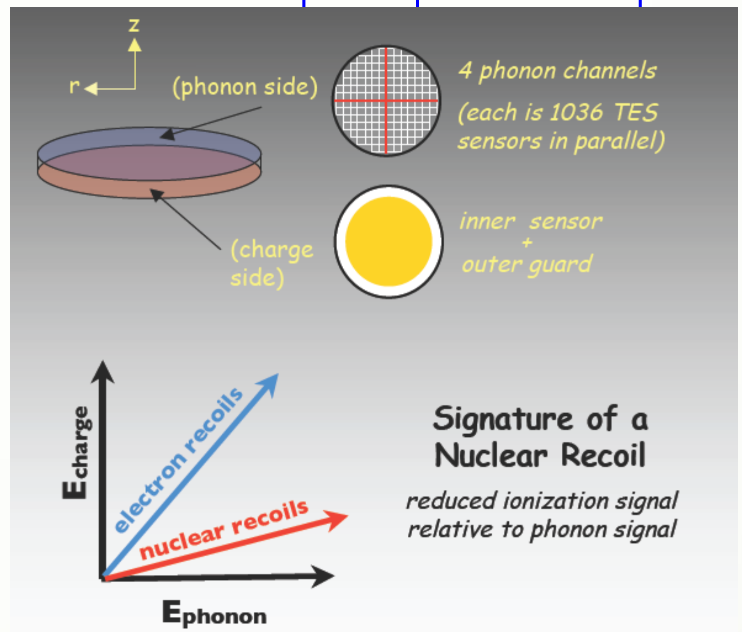

- Most backgrounds (e, γ) produce electron recoils
- WIMPS and neutrons produce nuclear recoils.
- Ionization yield (ionization energy per unit phonon energy) strongly depends on particle type.
- Particles that interact in the "surface dead layer" result in reduced ionization yield.

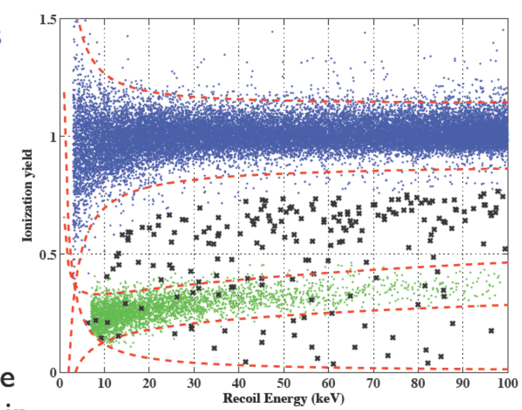

Double read-out bolometric technique (ion. vs heat)

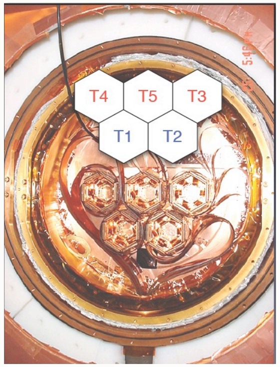

- CDMS-Ge: Soudan, 3.22 kg Ge, 194.1 kg x day; E_{th}=10 keV + other attemps at lower E_{th}
- SuperCDMS: Soudan, 9 kg Ge, 577 kg x day
- Edelweiss: LSM, 3.85 kg Ge, 384 kg x day; E_{th}=20 keV

  \+ search for low-mass WIMPs, ; E_{th}~1 keVee
- CDMS-Si: 1.2 kg Si, 140.2 kg x day; E_{th}=7 keV

Thermal sensors:
- superconductor thermistors (highly doped SC): NTD Ge → **EDELWEISS**
- superconducting transition sensors: TES → **CDMS**, **CRESST**

Towards low energy thresholds → **CDMSlite**: no charge collection, HV enhancement of the phonon signal (Neganov-Luke effect)

- **Many cuts on the data:** how about systematics?
- The **systematics** can be variable along the data taking period;
- **Poor detector performances:** many detectors excluded in the analysis
- **Critical stability of the performances**
- **Non-uniform** response of detector: intrinsic limit
- **Surface electrons:** PSD needed with related uncertainty

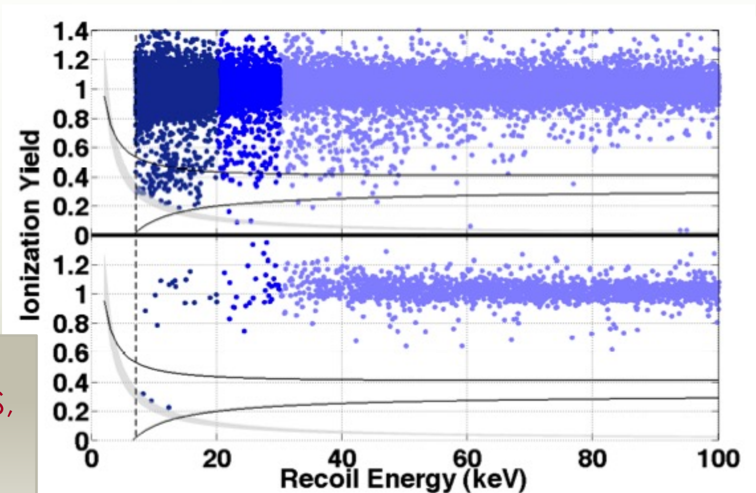

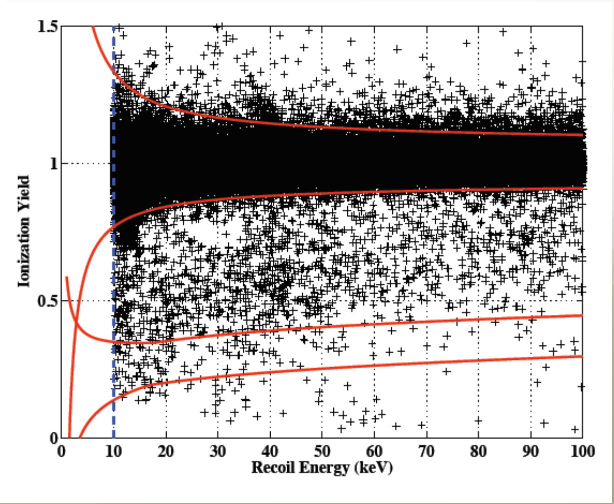

Anyhow, after many cuts few (two in CDMS-Ge, eleven in SuperCDMS, five in Edelweiss and three in CDMS-Si) events survive: positive hints or intrinsic limit reached?

Double read-out bolometric technique (scintillation vs heat)

Experimental site: Gran Sasso (LNGS)
Detector: 33 $CaWO_4$ crystals (10 kg mass)
data from 8 detectors
Exposure: ≈ 730 kg x day

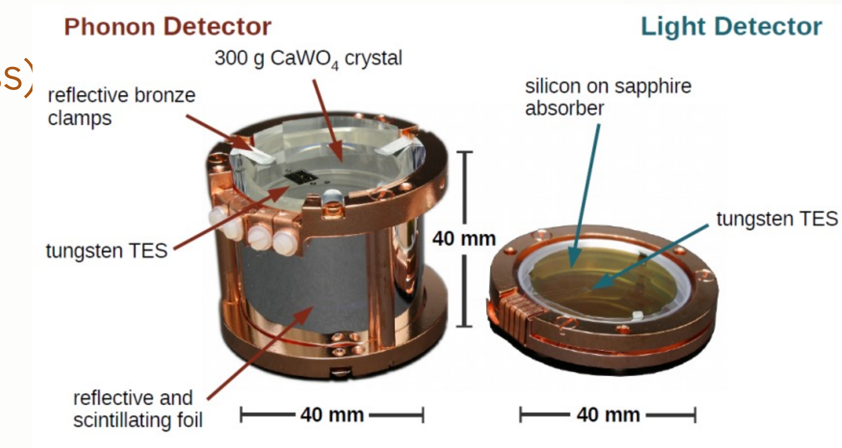

Discrimination of nuclear recoils from radioactive backgrounds by simultaneous measurement of phonons and scintillation light:

- Phonon: $CaWO_4$ crystals read out with TES
- Light: recorded by separate light detector also read out with TES

$$\text{Light Yield} = \frac{E_{\text{Light}}}{E_{\text{Phonon}}}$$

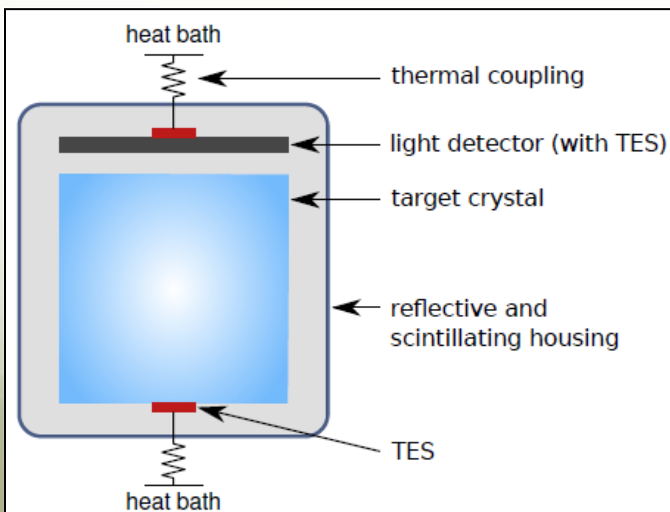

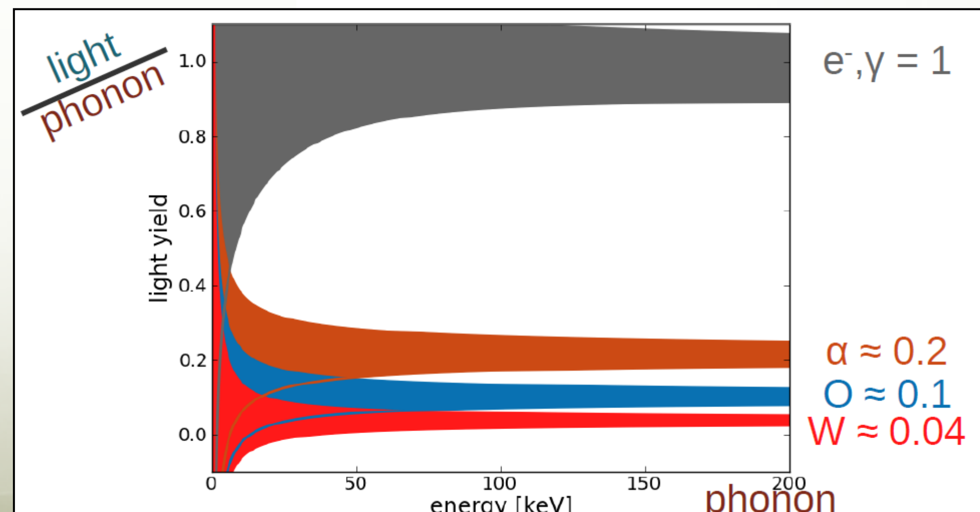

Double read-out bolometric technique (scintillation vs heat)

CRESST at LNGS: 33 $CaWO_4$ crystals (10 kg mass)
data from 8 detectors. Exposure: ≈ 730 kg x day

Data from one detector

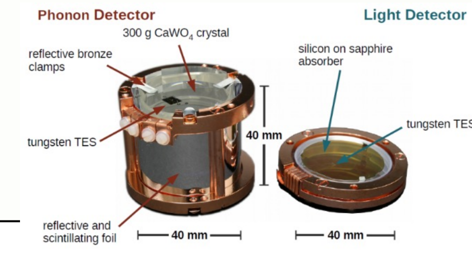

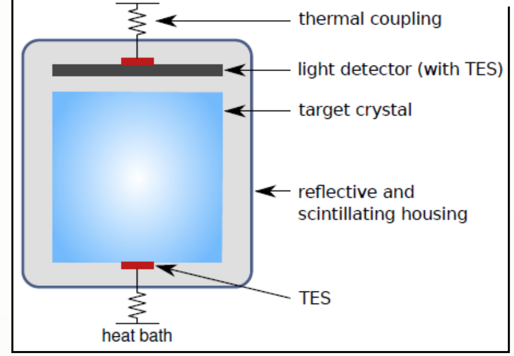

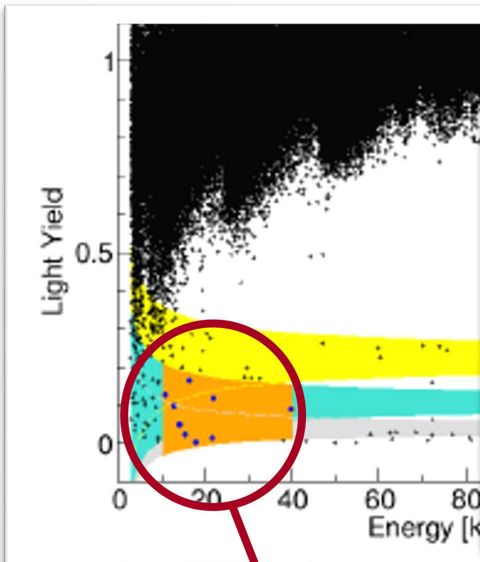

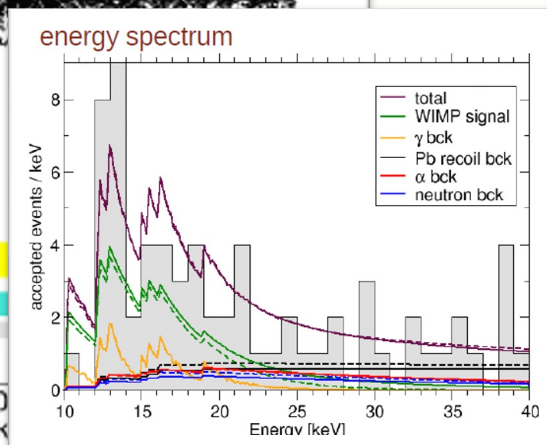

Efficiencies + stability + calibration, crucial role

67 total events observed in O-band

Systematics in previous runs (?):
Following run with lower exposure and lower energy threshold does not confirm this 3.5σ excess!!!

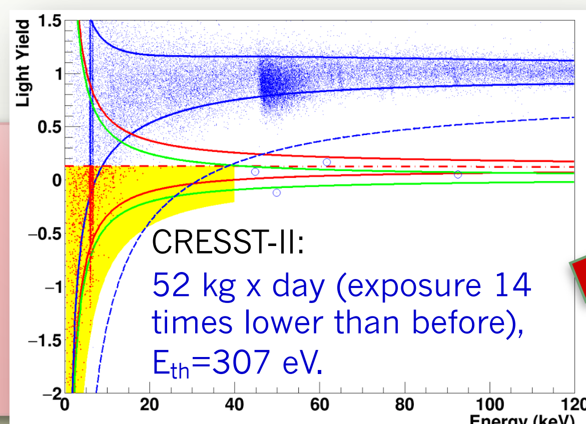

CRESST-II:
52 kg x day (exposure 14 times lower than before), E_{th}=307 eV.

CRESST-III (new detector modules, 24 g each, 100 eV thrs, 2.39 kg days)

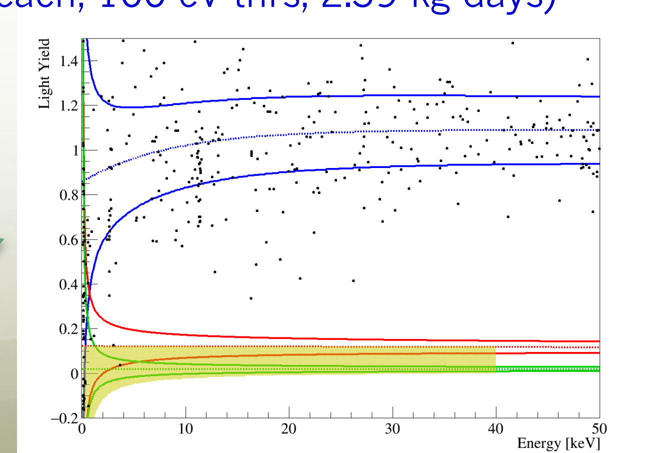

Positive hints from CoGeNT (ionization detector)

Experimental site: Soudan Underground Lab (2100 mwe)
Detector: 440 g, p-type point contact (PPC) Ge diode 0.5 keVee energy threshold
Exposure: 146 kg x day (dec '09 - mar '11)

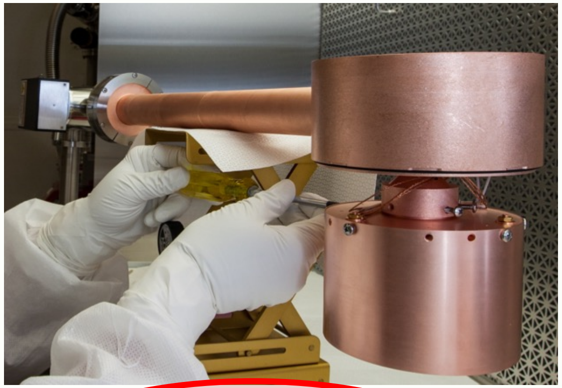

- ✓ **Irreducible excess** of bulk-like events below 3 keVee observed;

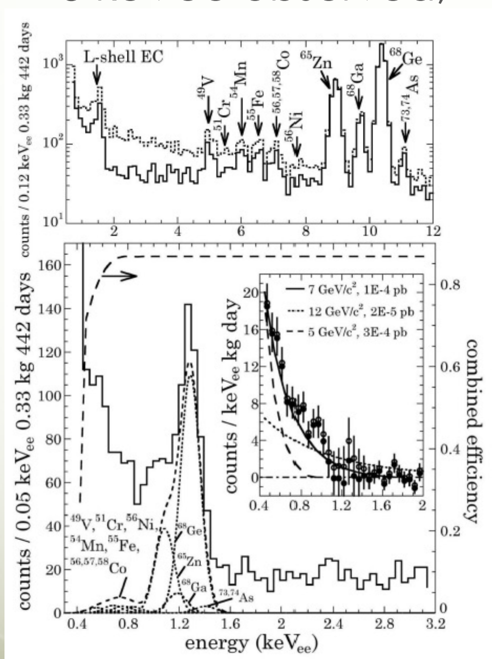

- ✓ **annual modulation** of the rate in 0.5-4.5 keVee at ~2.2σ C.L.

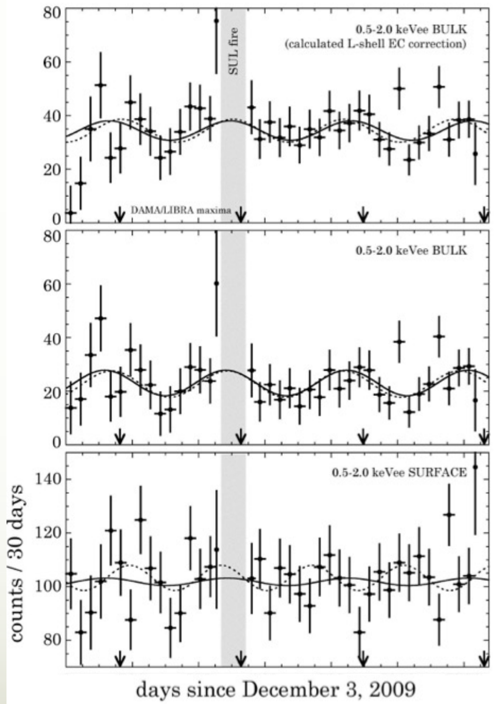

format. A straightforward analysis indicates a persistent annual modulation exclusively at low energy and for bulk events. Best-fit phase consistent with DAMA/LIBRA (small offset may be meaningful). Similar best-fit parameters to 15 mo dataset, but with much better bulk/surface separation (~90% SA for ~90% BR)

Unoptimized frequentist analysis yields ~2.2σ preference over null hypothesis. This however does not take into account the possible relevance of the modulation amplitude found...

Other Ge activity:
Texono, CDEX @ CJPL

- CoGeNT upgrade: C-4
- C-4 aims at x4 total mass increase, bckg decrease, and substantial threshold reduction. Soudan is still the lab

NaI(Tl) scintillating detectors

These experiments were motivated to reproduce the more-than-20-years DAMA results with its ULB NaI(Tl). They are at well different R&D stages. Intrinsically not enough sensitivity

ANAIS-112: 3×3 matrix of NaI(Tl) scintillators 12.5 kg each to study DM annual modulation at Canfranc (LSC); 1.5 yr of data taking released (exposure: 157.55 kg x yr)

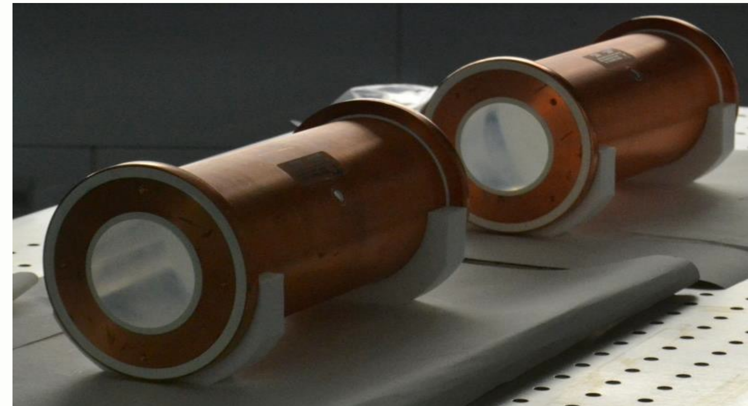

KIMS: CsI(Tl) crystals since 2000 at Yangyang (Y2L), Korea. Afterwards, KIMS-NaI joining Cosine

COSINE-100: ≈100 kg NaI in Y2L, released 1.7 years collected with five of the eight crystals (□60 kg) ⇒ 97.7 kg x yr.

Warning: PSD with CsI(Tl), NaI(Tl), ... sometimes overestimated sensitivity; claimed high rejection power, but existing systematics drastically limit the reachable sensitivity.

Key points: not only residual contaminants but also long-term/high-level stability, etc.

DM-ICE: NaI(Tl) deployed at the South Pole; exposure: 60.8 kg x yr

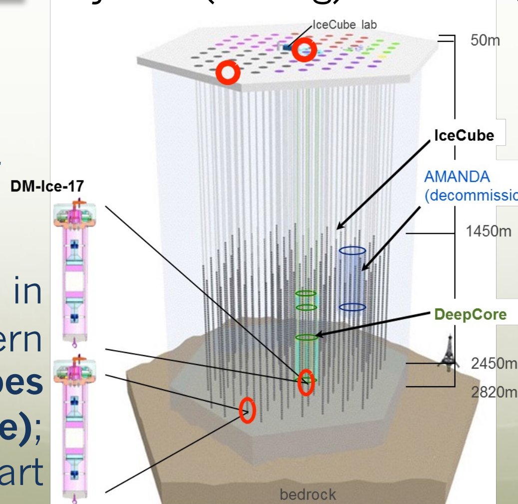

SABRE: two sites: LNGS in Northern and SUPL in Southern hemisphere **(but the effect does not depend on hemisphere)**; PoP (5 kg) ready to start

COSINUS: cryogenic calorimeters with pure NaI; dual readout; R&D phase 50 g to 300 g but scintillation different from standard temperature and doped conditions.

+ picoLON

DAMA/LIBRA-phase3: R&D under completion

Even very small **systematics** in the data selections and statistical discrimination and rejection procedures can be difficult to estimate;

e.m. component of the rate can contain the signal or part of it

Even assuming pure recoil case and ideal discrimination on an event-by-event base, the result will NOT be the identification of the presence of WIMP elastic scatterings as DM signal, because of the well **known existing recoil-like indistinguishable background**

*Therefore, even in the ideal case the "excellent suppression of the e.m. component of the counting rate" can **not** provide a "signal identification"*

A model independent signature is needed

Directionality Correlation of Dark Matter impinging direction with Earth's galactic motion due to the distribution of Dark Matter particles velocities

very hard to realize

Diurnal modulation Daily variation of the interaction rate due to different Earth depth crossed by the Dark Matter particles

only for high σ

Annual modulation Annual variation of the interaction rate due to Earth motion around the Sun

at present the only feasible one, sensitive to many DM candidates and scenarios

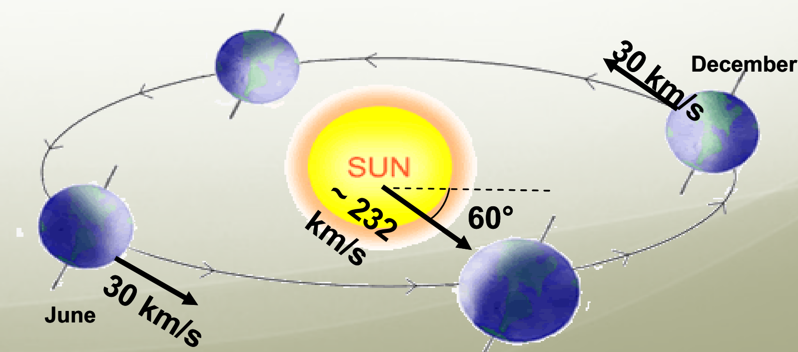

The annual modulation: a model independent signature for the investigation of DM particles component in the galactic halo

With the present technology, the annual modulation is the main model independent signature for the DM signal. Although the modulation effect is expected to be relatively small a suitable large-mass, low-radioactive set-up with an efficient control of the running conditions can point out its presence.

Drukier, Freese, Spergel PRD86; Freese et al. PRD88

Requirements of the annual modulation

1) Modulated rate according cosine
2) In a definite low energy range
3) With a proper period (1 year)
4) With proper phase (about 2 June)
5) Just for single hit events in a multi-detector set-up
6) With modulation amplitude in the region of maximal sensitivity must be <7% for usually adopted halo distributions, but it can be larger in case of some possible scenarios

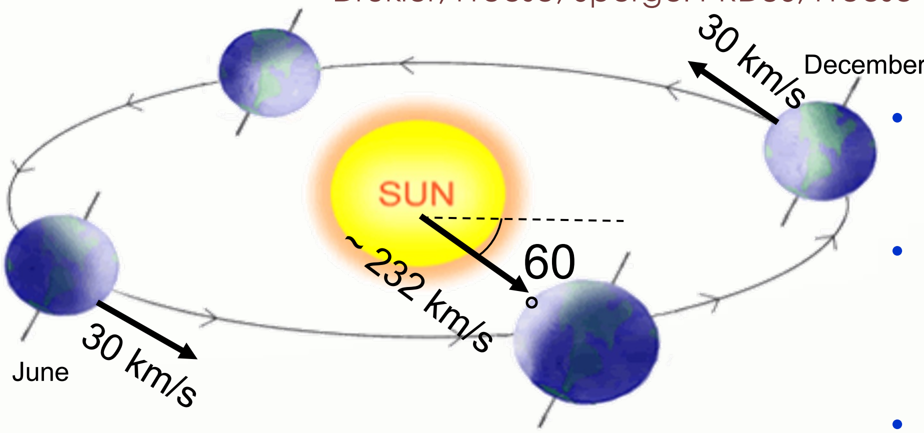

- v_{sun} ~ 232 km/s (Sun vel in the halo)
- v_{orb} = 30 km/s (Earth vel around the Sun)
- $\gamma = \pi/3$, $\omega = 2\pi/T$, T = 1 year
- $t_0 = 2^{nd}$ June (when $v_\oplus$ is maximum)

$$v_\oplus(t) = v_{sun} + v_{orb}\cos\gamma\cos[\omega(t-t_0)]$$

$$S_k[\eta(t)] = \int_{\Delta E_k} \frac{dR}{dE_R} dE_R \cong S_{0,k} + S_{m,k}\cos[\omega(t-t_0)]$$

the DM annual modulation signature has a different origin and peculiarities (e.g. the phase) than those effects correlated with the seasons

To mimic this signature, spurious effects and side reactions must not only - obviously - be able to account for the whole observed modulation amplitude, but also to satisfy contemporaneously all the requirements

A toy model on the velocity distribution

$$I(E_R) = \int_{v_{min}(E_R)}^{\infty} \frac{f(v)}{v} dv$$

The simplest velocity distribution for the galactic halo is given by the iso-thermal sphere where **f(v)** is a **Maxwellian** distribution

$$f(v)dv = \int_{\Omega} g(\vec{v})\, d^3v \quad \Rightarrow \quad g(\vec{w}) = \frac{1}{\pi^{3/2} v_0^3} e^{-\frac{w^2}{v_0^2}} \quad (\vec{w} = \vec{v} + \vec{v_E})$$

$$f(v) = \frac{2v^2}{\sqrt{\pi} v_0^3} e^{-\frac{v^2+v_E^2}{v_0^2}} \int_{-1}^{1} e^{-\frac{2 v v_E cos\vartheta}{v_0^2}} dcos\vartheta =$$

$$= \frac{v}{\sqrt{\pi} v_0 v_E} e^{-\frac{v^2+v_E^2}{v_0^2}} \left(e^{\frac{2vv_E}{v_0^2}} - e^{-\frac{2vv_E}{v_0^2}} \right)$$

$$= \frac{v}{\sqrt{\pi} v_0 v_E} \left(e^{-\frac{(v-v_E)^2}{v_0^2}} - e^{-\frac{(v+v_E)^2}{v_0^2}} \right)$$

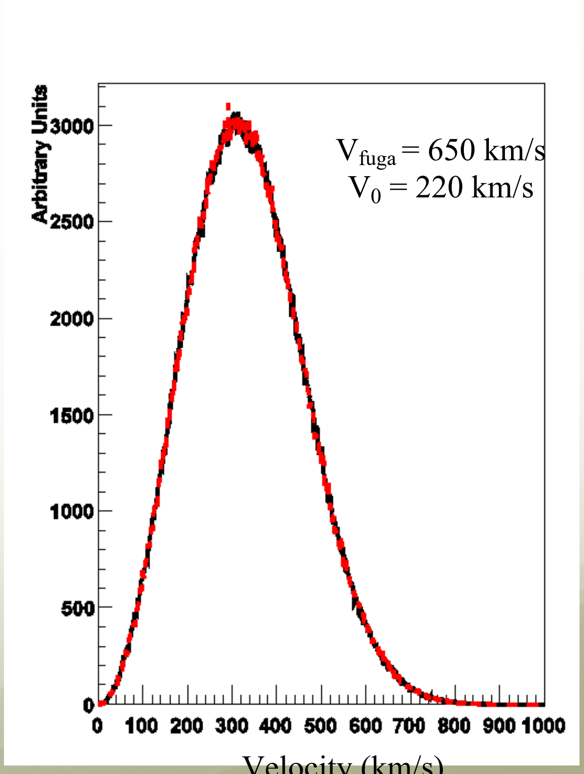

BUT: v_E is dependent on time (then, annual modulation of the signal)

The relative Earth speed along the galactic plane is given by:

$$v_E(t) \approx v_\odot + v_\oplus cos\gamma cos[\omega(t - t_0)]$$

Where:

- $v_\odot$ ~ 232 km/s (Sun velocity in the halo)
- $v_\oplus$ = 30 km/s (Earth velocity around the Sun)
- $\gamma = \pi/3$, $\omega = 2\pi/T$, T = 1 year and t_0 = 2nd June (when $v_\oplus$ is maximum)

We define: $$\eta(t) = \frac{v_E(t)}{v_0} = \eta_0 + \Delta\eta cos[\omega(t - t_0)]$$

Here $\Delta\eta << \eta_0$.

We can write R as a function of η and use Taylor expansion:

$$\frac{dR}{dE} \cong \left[\frac{dR}{dE}\right]_{\eta_0} + \frac{\partial}{\partial\eta}\left[\frac{dR}{dE}\right]_{\eta_0} \Delta\eta cos[\omega(t - t_0)]$$

Expected signal:

$$S_k[\eta(t)] = \int_{\Delta E_k} \frac{dR}{dE_R} dE_R \cong S_{0,k} + S_{m,k} \cos[\omega(t - t_0)]$$

where (energy bin ΔE_k):

$$\begin{cases} S_{0,k} = \dfrac{1}{\Delta E_k} \displaystyle\int_{\Delta E_k} \left[\dfrac{dR}{dE}\right]_{\eta_0} dE \\ S_{m,k} = \dfrac{1}{\Delta E_k} \displaystyle\int_{\Delta E_k} \dfrac{\partial}{\partial \eta} \left[\dfrac{dR}{dE}\right]_{\eta_0} \Delta\eta \, dE \end{cases}$$

In real experiment:
Several experimental parameters to be accounted for, such as energy resolution, q.f. in case DM candidates inducing just recoiling nuclei, etc.

DAMA set-ups

an observatory for rare processes @ LNGS

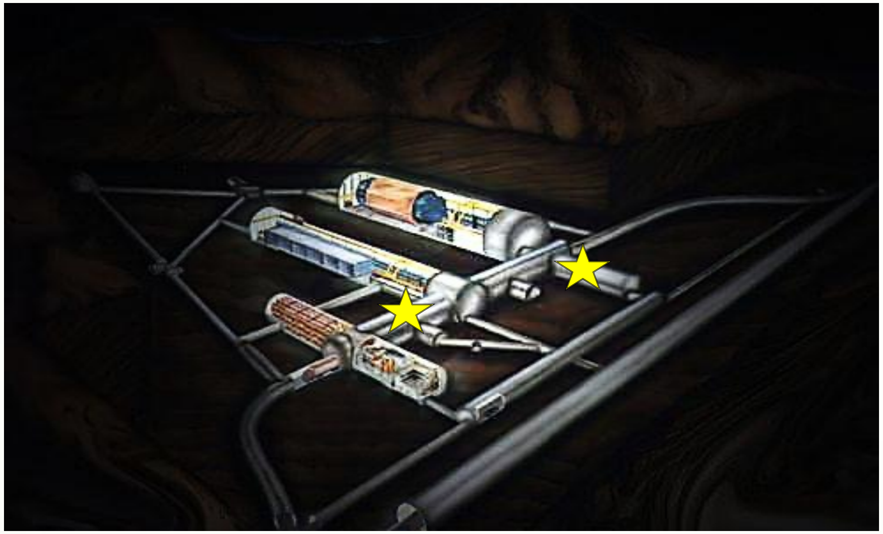

- DAMA/LIBRA (DAMA/NaI)
- DAMA/LXe
- DAMA/R&D
- DAMA/Crys
- DAMA/Ge

see the next lecture

Collaboration:

Roma Tor Vergata, Roma La Sapienza, LNGS, IHEP/Beijing

+ by-products and small scale expts.: INR-Kiev

+ neutron meas.: ENEA

+ in some studies on ββ decays (DST-MAE and Inter-Universities project):

IIT Kharagpur and Ropar, India